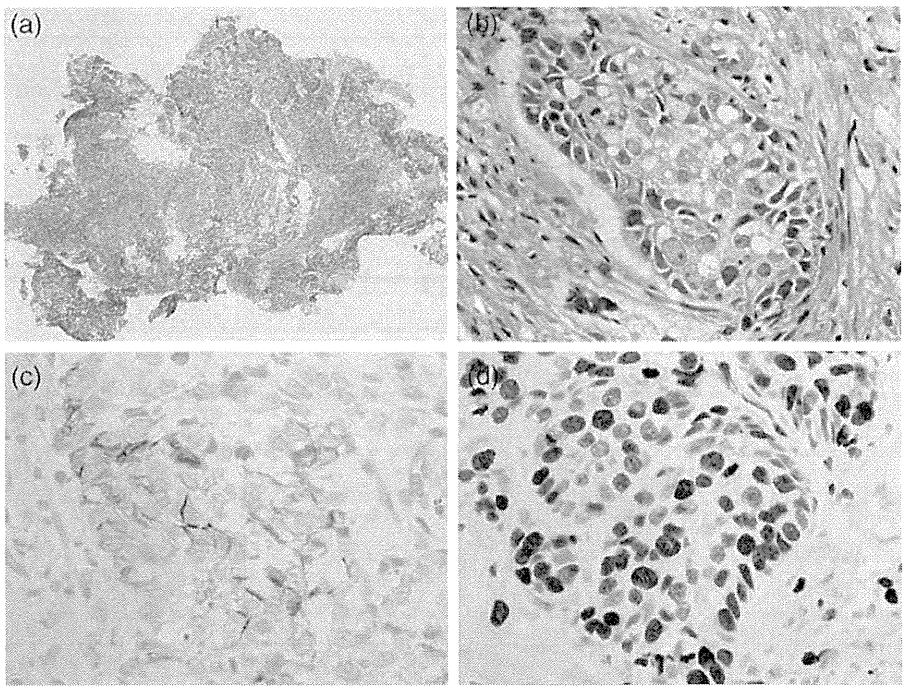

Figure 2. Morphological and immunohistochemical features of a biopsy specimen (Case 1). The low-powered view shows an irregular organoid nesting structure (a, H&E, ×4). In the high-powered view, the tumor consists of two types of cells, cells with nuclei with a fine chromatin pattern and larger cells with prominent nucleoli, and tumor cells show incomplete rosette and intercellular cleft formation (b, H&E, ×40). Immunohistochemically, NCAM (c, ×40) is positive and the Ki-67 labeling index is high (d, ×40).

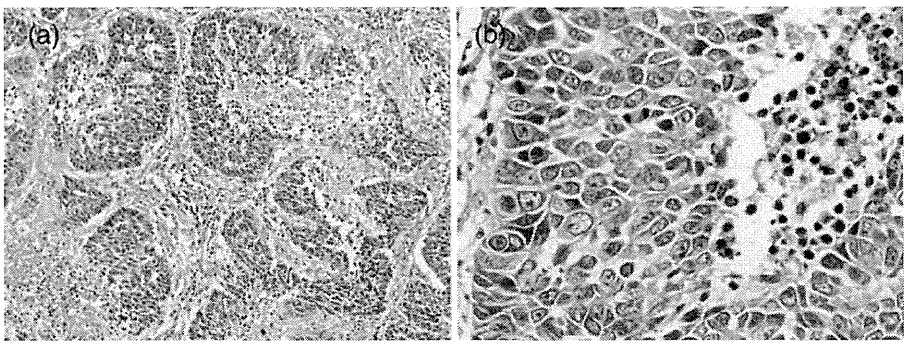

Figure 3. The morphology of a surgically resected tumor of Case 1. Tumor cells form an organoid nesting structure with necrosis (a, H&E, ×4) and show the features of non-small cell lung cancer with large nuclei with prominent nucleoli (b, H&E, ×40).

HNSCNECs. Among them, a fine nuclear chromatin pattern was the most frequent finding. These six biopsy specimens had a Ki-67/MIB1 labeling index from 56.6 to 98.7% (median: 70.6%).

The comparisons between histological findings of the biopsy specimen and the resected one in each case are shown in Fig. 4 and Table 5. Fine chromatin in biopsy specimens generally has changed to be rather course chromatin in resected specimens, and peripheral palisading, rosette formation, trabecular arrangement and organoid pattern have become clearly visible in four cases out of six.

DISCUSSION

Using our HNSCNEC criteria (9), we selected 38 cases from all lung biopsy specimens obtained in our hospital from 2002 to 2009. As shown in Table 2, various clinical characteristics of the 38 cases corresponded well with those of LCNEC cases, which have been already reported by many previous papers using surgically resected LCNEC (1,11–18). For example, CT findings have already revealed that LCNEC is peripherally located and has a solid mass with a lobulated margin (19). In this study, the serum pro-GRP level was elevated in 13 (35.1%) of 37 cases, but no report about the frequency of elevated serum pro-GRP in LCNEC has appeared in the literature. Previous investigations reported that the frequency of the elevated serum pro-GRP level is 68% in SCLC and 4.2% in NSCLC (20). The frequency of the elevated serum pro-GRP level might be low compared with that of SCLC.

The majority of the 38 cases had pathologically Stage IV disease and many patients died within 1 year after the lung

Table 5. Comparison of histological findings between biopsy specimen and resected ones (biopsy/resection) in Cases 1–6 in Table 2

Finding	Cytoplasm[a]	Nucleus[a]		Structure[a]					
	Wide	Fine chromatin	Nucleolar prominence	Peripheral palisading	Rosettes	Trabecular	Organoid	Discohesive	Necrosis
Case 1*	2/1	2/0[b]	2/2	2/1	2/2	0/0	3/3	1/3	0/2
Case 2	1/1	2/1	1/2	1/3	1/1	0/3	1/3	1/1	0/0
Case 3**	1/2	2/0	2/2	0/0	0/3	0/1	0/1	0/1	0/1
Case 4	2/2	2/1	1/2	0/0	1/2	0/0	1/3	1/0	2/1
Case 5**	2/3	3/1	0/2	0/2	0/1	0/1	0/2	3/1	2/2
Case 6	3/3	3/1	0/1	0/0	0/0	0/0	1/2	1/0	0/1

[a]Each numeral indicates: [b]0, not observed; 1, partially or focally observed; 2, easily and/or widely observed; 3, remarkably observed. Underline indicates that a difference of 2 or 3 degrees exists between evaluation numerals of biopsy specimen and resected one.
*Findings shown in Figs 2 and 3.
**Findings shown in Fig. 4.

biopsy in this study. LCNEC is a highly malignant neoplasm and previous comparative studies using surgically resected high-grade neuroendocrine carcinoma cases revealed that the prognosis of LCNEC is similar to that of SCLC (16,18,21). Of the 38 cases in this study, 6 were clinical TNM Stage I, II or IIIA, which then underwent surgery after biopsy and the diagnosis was pathologically confirmed as LCNEC using surgically resected tumor specimens. These findings suggest that our HNSCNEC criteria are applicable in practical use for the diagnosis of LCNEC using biopsy specimens.

Among high-grade neuroendocrine carcinoma of the lung, the overall clinicopathological features of LCNEC, including unresectable cases, is still uncertain compared with those of SCLC (22). As it is extremely difficult to make a final diagnosis of LCNEC using only biopsy and/or cytology specimens, the true frequency of LCNEC is undetermined. As the results of a study using surgically resected LCNEC cases, the frequency has been reported to be 1.6–3.1% (7,11,13). If all 38 cases in our study were compatible with LCNEC, the true frequency of LCNEC would be 3.7% (38 out of 1040 biopsies). In the Japanese lung cancer registry study using a large number of surgical and non-surgical cases in 2002, the proportions of adenocarcinoma, squamous cell carcinoma and small cell carcinoma were 56.7, 25.7 and 9.2%, respectively (23). In our biopsy series, these proportions were 49.8, 30.6 and 11.6%, which showed a similar tendency to those of the Japanese lung cancer registry study, although the number is small; therefore, the real frequency of LCNEC might be over 3.7%.

In 1991, Travis et al. (1) proposed a category of LCNEC that was adopted in the WHO classification of lung cancer in 1999 and 2004 (2,3); however, these criteria are applicable only to surgically resected specimens, not to biopsy specimens. Biopsy specimens are too small to have enough morphological information and to count the number of mitoses; therefore, we modified the WHO criteria of LCNEC and proposed new criteria for diagnosing LCNEC using biopsy specimens (9). In our criteria, the immunohistochemical Ki-67/MIB1 labeling index was used instead of the mitotic count. Our study clearly showed that it was very difficult or impossible to count mitoses in small biopsy specimens, but immunohistochemical Ki-67/MIB1 labeling indices could be useful for evaluating the proliferation activity. Fortunately, for 7 of 38 biopsy specimens the number of mitoses could be counted and these specimens were elucidated to have more proliferative activity than biopsy specimens with an impossible mitosis count. In Stage I NSCLCs, the mean Ki-67/MIB1 labeling index is 19.3% (24), and the prognosis of NSCLC patients is reported to differ between the '20% or higher' group and the 'lower than 20%' group of the Ki67/MIB1 labeling index (25). When compared with the positivity of the Ki-67/MIB1 labeling index of NSCLC, the labeling index of our biopsy specimens in this study was quite high, which suggests that high proliferative activity is one of the characteristic features of LCNEC (26).

In the WHO criteria, large cell morphology is one of the most important criteria for LCNEC, such as large tumor cell size with abundant cytoplasm as well as vesicular nuclei and prominent nucleoli (2,3). Our criteria of HNSCNEC (9) also followed the WHO criteria; however, the recognition of this large cell morphology is problematic among pathologists. In previously published papers discussing the interobserver variability of SCLC and LCNEC, the cytologic features of a nuclear/cytoplasmic ratio may be recognized arbitrarily or not quantitatively among diagnostic pathologists (4,5,17,27). It is also reported that there are borderline cases between LCNEC and SCLC in high-grade neuroendocrine carcinoma (17). In this study, about one-third of cases were diagnosed as high-grade neuroendocrine carcinoma, but there was a hesitation to diagnose them as LCNEC, because of the cytological similarity to SCLC. Previous studies using surgically resected tumors revealed that LCNEC and SCLC have distinct characteristic morphological features; namely, a large tumor cell size, peripheral palisading and prominent nucleoli

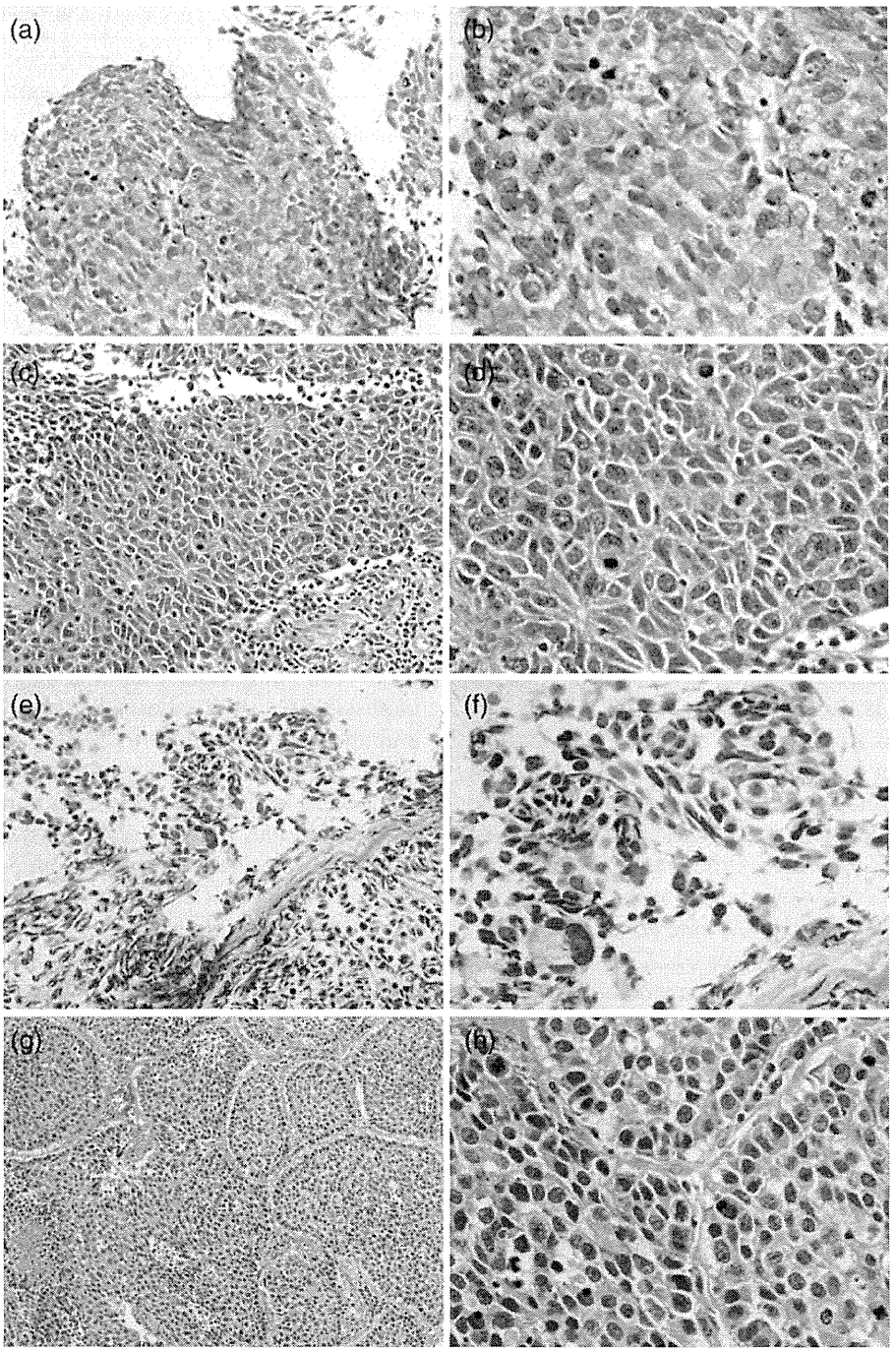

Figure 4. Histological comparison between biopsy and resected specimens in two of the resected six cases. In Case 3 (a–d), the biopsy specimen shows fine chromatin architecture with visible nucleoli and an obscure rosette pattern (a, H&E, ×20; b, H&E, ×40). However, in the resected specimen, a large number of rosettes are observed (c, H&E, ×20; d, H&E, ×40). The chromatin is coarse and the cytoplasm is abundant. In Case 5 (e–h), the biopsy specimen is crushed and neither the neuroendocrine structure nor nucleoli can be recognized (e, H&E, ×20; f, H&E, ×40). However, in the resected specimen, peripheral palisading, organoid nesting and nucleoli are clearly observed (g, H&E, ×10; h, H&E, ×40).

are characteristic of LCNEC, and a small cell size, high nuclear/cytoplasmic ratio and fine chromatin pattern are characteristic findings of SCLC (1–3,17,18); however, these morphological features are known to overlap among LCNEC and SCLC (1,17,18). As shown in Table 3, morphological analysis of 38 biopsy specimens revealed that the incidence of the specimen with a fine chromatin pattern was the highest, and those with intracellular cleft and prominent nucleoli followed in a decreasing order. Therefore, the morphological fine chromatin pattern is not only seen in surgically resected SCLC, but is also a characteristic finding of LCNEC in biopsy specimens as shown in Figs 2 and 4, Tables 3 and 5. Even in surgically resected LCNEC, the appearance of tumor cells with fine nuclear chromatin has been

Table 6. Comparison among diagnostic criteria of WHO (3), our former proposal (9) and the present study for LCNEC

Findings	WHO 2004 (3)	Igawa et al. (9)	Present study
Applied specimen	Resected	Biopsy	Biopsy
Differentiation			
Histological differentiation without SCLC morphology, glandular and squamous differentiation	EA, Ess	EA, Ess	EA, Ess
Cell size			
Large cell size and low nuclear/cytoplasmic ratio	EA, Ess	EA, Ess	EA, Ess
Neuroendocrine differentiation			
Immunostain positive for at least one of neuroendocrine markers	EA, Ess	EA, Ess	EA, Ess
Proliferating activity			
Mitosis (11 or greater/mm^2)	EA, Ess	DA	DA, nd
Ki67/MiB-1 labeling index (>40%)	nd	EA, Ess	EA, Ess
Nuclear findings			
Nucleoli (frequent and prominent)	EA, LS	EA, LS	EA, LS
Chromatin pattern (vesicular, coarse or fine)[a]	EA, Ess (vesicular or coarse chromatin pattern is common)	EA, Ess	EA (fine chromatin pattern is common)
Neuroendocrine morphology			
Organoid nesting, palisading and rosettes, trabecular	EA, Ess	CA, SF	CA, SF
Others			
Necrosis	EA, common	CA, SF	CA, SF
Cellular atypia	nd	Moderate to severe, Ess	nd
Intercellular space (cleft)	nd	EA, SF	EA, SF

LCNEC, large cell neuroendocrine carcinoma; SCLC, small cell lung carcinoma; EA, easily assessed; Ess, essential; DA, difficult to be assessed; nd, not determined, LS, lacking sometimes; CA, can be assessed sometimes; SF, supportive findings.
[a]Ref. (2) and Table 1.08 in ref. (3).

noted (1,18). As our resected cases were found to show a chromatin pattern changed from the fine pattern in the biopsy specimen to a coarse or vesicular pattern (Fig. 4 and Table 5), it is supposed that the different fixative conditions might have some effects on the chromatin morphology of tumor cells. The greatest difference might be due to a rapid start and full immersion in formalin soon after taking a biopsy specimen, in contrast to a delayed start and immersion in a relatively small ratio of fixative amount/specimen size for a resected specimen, resulting in fine chromatin morphology and a coarse or vesicular one, respectively. Furthermore, as another histological finding, intercellular cleft might reflect poor intercellular connection and might be one of the characteristics of LCNEC.

In LCNEC, the appearance of neuroendocrine morphology such as organoid nesting, palisading, rosette and trabeculae has been frequently observed and their frequencies are reported to be 90.9, 59.1, 72.7 and 31.8%, respectively (18). In contrast, Figs 2 and 4 revealed that the neuroendocrine morphology was relatively difficult to recognize in biopsy specimens. This may be attributed to the small size of specimens. Therefore, immunohistochemical detection of a neuroendocrine marker is a more reliable method to identify the neuroendocrine features of biopsy specimens. In a previous report, synaptophysin was frequently positive at the rate of 77% in LCNEC, and chromogranin A and CD56 followed (17). In our study, NCAM was the most frequently immunopositive neuroendocrine marker and chromogranin A followed after synaptophysin. This may be explained by the difference of the pattern of immunostaining because NCAM tends to stain tumor cells diffusely compared with chromogranin A or synaptophysin. For immunohistochemical evaluation of neuroendocrine features in both surgically resected or biopsy samples, immunohistochemistry using three neuroendocrine markers is necessary.

Although the cases in the early stage can be resected and histologically confirmed, the cases in an advanced stage should receive chemotherapy without histologically examining resected specimens. Then the criteria of HNSCNEC may give the chance for lesions that have the possibility of being LCNEC to be treated as inoperable advanced probable LCNEC cases. For this reason some papers have reported that the clinical efficacy of chemotherapy for LCNEC is comparable with that for SCLC (7–10); the diagnosis of

Table 7. Proposed diagnostic criteria for possible LCNEC using biopsy specimens

Major points
1. Poorly differentiated NSCLC with neither acinar nor squamous differentiation
(a) Tumor cell contains a nucleus larger than the size of three small resting lymphocytes, and low nuclear/cytoplasmic ratio or abundant cytoplasm
(b) Tumor nucleus with a fine chromatin pattern and/or prominent nucleoli
2. Ki-67/MIB1 labeling index >40%
3. Positive immunostaining for one or more neuroendocrine markers (NCAM, chromogranin A and synaptophysin)
Minor points
1. Neuroendocrine morphology (organoid nesting, peripheral palisading[a], rosettes, trabecular architecture)
2. Frequent massive necrosis
3. Intercellular space (cleft) or discohesiveness

[a]Peripheral palisading is mentioned as 'basal palisading' in Table 1; both stand for a similar finding.

HNSCNEC as a surrogate of LCNEC or as a probable LCNEC would help these lesions to receive more appropriate therapy. When the criteria of HNSCNEC work, the number of patients who receive chemotherapy for LCNEC, comparable to that for SCLC, might increase by 0.6–2.1% of the number of all lung carcinomas. This estimation is according to the comparison between the reported frequency (1.6–3.1%) of LCNEC (7,11,13) and the incidence (3.7%, 38 out of 1040 lung biopsies positive for cancer) of HNSCNEC in our hospital, which has already been discussed.

WHO criteria (3), our previous criteria (9) and our new criteria have three common essential points as indicated in the upper one-third of Table 6; and there is one more essential point on proliferating activity. In our new criteria, the Ki67/MIB1 labeling index is adopted instead of mitotic counting. Then our new criteria can be shown as in Table 7. Summarizing the data obtained in this study using biopsy specimens, we simplified our previous criteria for HNSCNEC and proposed new diagnostic criteria suitable for possible LCNEC (28). In the new criteria (Table 7), the major points are essential for diagnosing LCNEC using biopsy specimens. In addition to the major points, the findings due to additional minor points would increase the possibility of an LCNEC diagnosis. We expect these new criteria to be used in routine surgical pathology and to facilitate the clinicopathological study of high-grade neuroendocrine carcinoma, especially LCNEC.

Acknowledgements

The authors would like to thank Mrs The authors thank Minako Ishii for her support.

Funding

This study was supported by a grant from the Ministry of Health, Labor and Welfare (JCOG0007-A) in Japan.

Conflict of interest statement

None declared.

References

1. Travis WD, Linnoila RI, Tsokos MG, et al. Neuroendocrine tumors of the lung with proposed criteria for large-cell neuroendocrine carcinoma. An ultrastructural, immunohistochemical, and flow cytometric study of 35 cases. *Am J Surg Pathol* 1991;15:529–53.
2. Travis WD, Colby TV, Corrin B, Shimosato Y, Brambilla E, editors. *World Health Organization International Histological Classification of Tumours: Histological Typing of Lung and Pleural Tumours*, 3rd edn. Berlin: Springer 1999.
3. Travis WD, Brambilla E, Müller-Hermelink HK, Harris CC, editors. *World Health Organization Classification of Tumours. Pathology and Genetics: Tumours of the Lung, Pleura, Thymus and Heart*. Lyon: IARC 2004.
4. Travis WD, Gal AA, Colby TV, Klimstra DS, Falk R, Koss MN. Reproducibility of neuroendocrine lung tumor classification. *Hum Pathol* 1998;29:272–9.
5. Den Bakker MA, Willemsen S, Grünberg K, et al. Small cell carcinoma of the lung and large cell neuroendocrine carcinoma interobserver variability. *Histopathology* 2010;56:356–63.
6. Iyoda A, Hiroshima K, Toyozaki T, et al. Adjuvant chemotherapy for large cell carcinoma with neuroendocrine features. *Cancer* 2001;92:1108–2.
7. Rossi G, Cavazza A, Marchioni A, et al. Role of chemotherapy and the receptor tyrosine kinases KIT, PDGFRα, PDGFRβ, and met in large-cell neuroendocrine carcinoma of the lung. *J Clin Oncol* 2005;23:8774–85.
8. Iyoda A, Hiroshima K, Moriya Y, et al. Prospective study of adjuvant chemotherapy for pulmonary large cell neuroendocrine carcinoma. *Ann Thorac Surg* 2006;82:1802–7.
9. Igawa S, Watanabe R, Ito I, et al. Comparison of chemotherapy for unresectable pulmonary high-grade non-small cell neuroendocrine carcinoma and small-cell lung cancer. *Lung Cancer* 2010;68:438–45.
10. Shimada Y, Niho S, Ishii G, et al. Clinical features of unresectable high-grade lung neuroendocrine carcinoma diagnosed using biopsy specimens. *Lung Cancer* 2012;75:368–73.
11. Jiang SX, Kameya T, Shoji M, Dobashi Y, Shinada J, Yoshimura H. Large cell neuroendocrine carcinoma of the lung: a histologic and immunohistochemical study of 22 cases. *Am J Surg Pathol* 1998;22:526–37.
12. Iyoda A, Hiroshima K, Toyozaki T, Haga Y, Fujisawa T, Ohwada H. Clinical characterization of pulmonary large cell neuroendocrine carcinoma and large cell carcinoma with neuroendocrine morphology. *Cancer* 2001;91:1992–2000.
13. Takei H, Asamura H, Maeshima A, et al. Large cell neuroendocrine carcinoma of the lung: a clinicopathologic study of eighty-seven cases. *J Thorac Cardiovasc Surg* 2002;124:285–92.
14. Paci M, Cavazza A, Annessi V, et al. Large cell neuroendocrine carcinoma of the lung: a 10-year clinicopathologic retrospective study. *Ann Thorac Surg* 2004;77:1163–7.
15. Battafarano RJ, Fernandez FG, Ritter J, et al. Large cell neuroendocrine carcinoma: an aggressive form of non-small cell lung cancer. *J Thorac Cardiovasc Surg* 2005;130:166–72.
16. Asamura H, Kameya T, Matsuno Y, et al. Neuroendocrine neoplasms of the lung: a prognostic spectrum. *J Clin Oncol* 2006;24:70–6.
17. Hiroshima K, Iyoda A, Shida T, et al. Distinction of pulmonary large cell neuroendocrine carcinoma from small cell lung carcinoma: a morphological, immunohistochemical, and molecular analysis. *Mod Pathol* 2006;19:1358–68.
18. Sun L, Sakurai S, Sano T, Hironaka M, Kawashima O, Nakajima T. High-grade neuroendocrine carcinoma of the lung: comparative

clinicopathological study of large cell neuroendocrine carcinoma and small cell lung carcinoma. *Pathol Int* 2009;59:522–9.
19. Oshiro Y, Kusumoto M, Matsuno Y, et al. CT findings of surgically resected large cell neuroendocrine carcinoma of the lung in 38 patients. *Am J Roentgenol* 2004;182:87–91.
20. Goto K, Kodama T, Hojo F, et al. Clinicopathological characteristics of patients with nonsmall cell lung carcinoma with elevated serum progastrin-releasing peptide levels. *Cancer* 1998;82:1056–61.
21. Iyoda A, Hiroshima K, Baba M, Saitoh Y, Ohwada H, Fujisawa T. Pulmonary large cell carcinoma with neuroendocrine features are high-grade neuroendocrine tumors. *Ann Thorac Surg* 2002;73:1049–54.
22. Nicholson SA, Beasley MB, Brambilla E, et al. Small cell lung carcinoma (SCLC): a clinicopathologic study of 100 cases with surgical specimens. *Am J Surg Pathol* 2002;26:1184–97.
23. Sawabata N, Asamura H, Goya T, et al. Japanese lung cancer registry study: first prospective enrollment of a large number of surgical and nonsurgical cases in 2002. *J Thorac Oncol* 2010;5:1369–75.
24. Haga Y, Hiroshima K, Iyoda A, et al. Ki-67 expression and prognosis for smokers with resected stage I non-small cell lung cancer. *Ann Thorac Surg* 2003;75:1727–32.
25. Shiba M, Kohno H, Kakizawa K, et al. Ki-67 immunostaining and other prognostic factors including tobacco smoking in patients with resected nonsmall cell lung carcinoma. *Cancer* 2000;89:1457–65.
26. Iyoda A, Hiroshima K, Moriya Y, et al. Pulmonary large cell neuroendocrine carcinoma demonstrates high proliferative activity. *Ann Thorac Surg* 2004;77:1891–5.
27. Marchevsky AM, Gal AA, Shah S, Koss MN. Morphometry confirms the presence of considerable nuclear size overlap between 'small cells' and 'large cells' in high-grade pulmonary neuroendocrine neoplasms. *Am J Clin Pathol* 2001;116:466–72.
28. Travis WD, Brambilla E, Noguchi M, et al. International association for the study of lung cancer/American Thoracic Society/European Respiratory Society international multidisciplinary classification of lung adenocarcinoma. *J Thorac Oncol* 2011;6:244–85.

analytical chemistry

Article

pubs.acs.org/ac

Microcavity Array System for Size-Based Enrichment of Circulating Tumor Cells from the Blood of Patients with Small-Cell Lung Cancer

Masahito Hosokawa,[†,‡] Takayuki Yoshikawa,[†] Ryo Negishi,[†] Tomoko Yoshino,[†] Yasuhiro Koh,[‡] Hirotsugu Kenmotsu,[§] Tateaki Naito,[§] Toshiaki Takahashi,[§] Nobuyuki Yamamoto,[§] Yoshihito Kikuhara,[⊥] Hisashige Kanbara,[⊥] Tsuyoshi Tanaka,[†] Ken Yamaguchi,[‡] and Tadashi Matsunaga*[,†]

[†]Division of Biotechnology and Life Science, Institute of Engineering, Tokyo University of Agriculture and Technology, Koganei, Japan

[‡]Drug Discovery and Development Division, Shizuoka Cancer Center Research Institute, Nagaizumi-cho, Sunto-gun, Japan

[§]Division of Thoracic Oncology, Shizuoka Cancer Center, Nagaizumi-cho, Sunto-gun, Japan

[⊥]Hitachi Chemical Co., Ltd, Shinjuku-ku, Japan

Supporting Information

ABSTRACT: In this study, we present a method for efficient enrichment of small-sized circulating tumor cells (CTCs) such as those found in the blood of small-cell lung cancer (SCLC) patients using a microcavity array (MCA) system. To enrich CTCs from whole blood, a microfabricated nickel filter with a rectangular MCA (10^4 cavities/filter) was integrated with a miniaturized device, allowing for the isolation of tumor cells based on differences in size and deformability between tumor and blood cells. The shape and porosity of the MCA were optimized to efficiently capture small tumor cells on the microcavities under low flow resistance conditions, while allowing other blood cells to effectively pass through. Under optimized conditions, approximately 80% of SCLC (NCI-H69 and NCI-H82) cells spiked in 1 mL of whole blood were successfully recovered. In clinical samples, CTCs were detectable in 16 of 16 SCLC patients. In addition, the number of leukocytes captured on the rectangular MCA was significantly lower than that on the circular MCA ($p < 0.001$), suggesting that the use of the rectangular MCA diminishes a considerable number of carryover leukocytes. Therefore, our system has potential as a tool for the detection of CTCs in small cell-type tumors and detailed molecular analyses of CTCs.

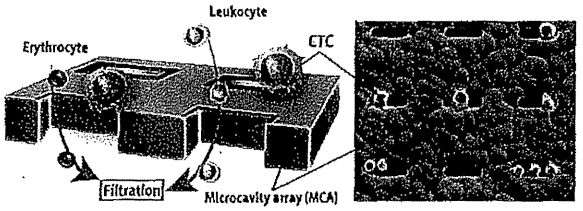

Circulating tumor cells (CTCs) are defined as tumor cells circulating in the peripheral blood of patients with metastatic cancer. The number of CTCs in peripheral blood has prognostic value in patients and can be used to evaluate therapeutic effects.[1,2] Furthermore, molecular analysis of CTCs provides valuable information for the characterization of CTCs and understanding cancer metastasis.[3,4] Detection of abnormal genes in CTCs can also contribute to the planning of personalized medicine using molecular-targeted drugs.[5,6] However, as CTCs are extremely rare (1 in 10^9 blood cells), enrichment is required to increase detection sensitivity to an acceptable level. The most often used CTC enrichment technique is immunomagnetic separation, which uses magnetic beads coated with monoclonal antibodies that target an epithelial cell marker such as EpCAM to enrich CTCs.[7,8] However, several studies have shown that the presence of EpCAM on tumor cells varies with tumor type.[9,10] The expression of various epithelial cell markers such as EpCAM is down-regulated to increase the invasiveness and metastatic potential via the epithelial-to-mesenchymal transition.[11−14] It has been suggested that the lower detection of CTCs with the CellSearch system (Veridex, Raritan, NJ), which is a semi-automated immunomagnetic separation system, in patients with advanced nonsmall-cell lung cancer (NSCLC) may be due to the loss of EpCAM expression.[15] Therefore, CTC enrichment methods based on an antigen−antibody reaction cannot isolate CTCs stably or reproducibly from all tumor types.

Other groups have reported CTC separation methods based on differences in size and deformability between CTCs and hematologic cells. Isolation by size of epithelial tumor cells (ISET) can be achieved by filtration because tumor cells (>8 μm) are larger than leukocytes.[16−19] ISET using a polycarbonate filter is an inexpensive, user-friendly method for enriching CTCs, as it enables the enrichment of EpCAM negative CTCs on the basis of size. CTC detection sensitivity with ISET in clinical tests of patients with metastatic lung cancer has been previously reported as higher than that with a conventional EpCAM expression-based CellSearch System.[20−22]

Recently, microfabricated devices for size-based separation of tumor cells have been developed to enable efficient enrichment of CTCs.[23−28] We have also developed a miniaturized

Received: January 17, 2013
Accepted: May 24, 2013
Published: May 24, 2013

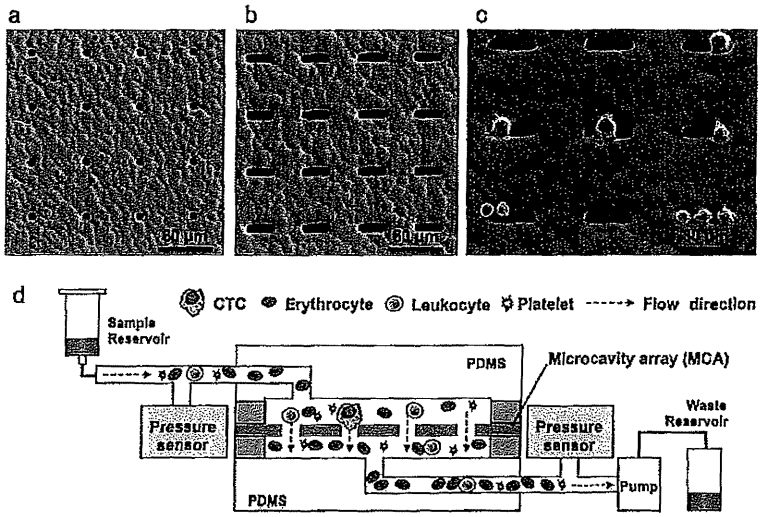

Figure 1. MCA for size-based isolation of circulating tumor cells. (a) SEM image of the circular MCA. (b) SEM image of the rectangular MCA. (c) SEM image of NCI-H69 cells trapped on the rectangular MCA. (d) Schematic image of the CTC enrichment device.

microcavity array (MCA) system for highly efficient enrichment of cells based on differences in cell size.[29−31] In this system, use of a miniaturized device allowed for the introduction of a series of reagents through the microfluidic structure for the detection of tumor cells. The shapes and sizes of the circular microcavities were designed to trap tumor cells, while allowing blood cells to flow through during whole blood filtration. Using a circular microcavity with an 8 μm diameter, the detection efficiency of NSCLC cells in a 1 mL blood sample spiked with 10−100 cells was approximately 96%. Our recent clinical study showed that the circular MCA system might be superior to the CellSearch System for detecting CTCs in patients with NSCLC and small-cell lung cancer.[32]

Although some studies have described morphological variations in tumor cells, little is known about the morphological features of CTCs.[33] It was reported that a portion of the CTCs detected in the blood of a patient with colorectal cancer were the same size as or smaller than leukocytes, whereas the majority of CTCs were larger than benign leukocytes.[34] In addition, the size of the CTCs detected by the CellSearch System and ISET differed significantly. In a study of lung cancer patients, Krebs et al. reported that the size range of cells estimated by CellSearch was 4−18 μm and that measured by ISET was 12−30 μm.[15] Moreover, CTC clusters, defined as contiguous clusters of cells containing 3 or more nuclei, were observed by ISET in 38% of the patients examined, whereas CellSearch detected no CTC clusters. These results indicate that the immunomagnetic separation techniques cannot isolate large clusters (20−130 μm), and ISET lost small CTCs, which include cells with features suggestive of apoptosis, such as irregular nuclear or cytoplasmic condensation or frank fragmentation into dense rounded structures.

In this study, we further optimized the structure of MCA for enrichment of small-sized tumor cells such as those found in small-cell lung cancer (SCLC). We developed a rectangular MCA by electroforming to improve the number and purity of small tumor cells recovered from whole blood. Using this MCA, we conducted a clinical test for the enrichment and detection of CTCs from the blood of patients with metastatic SCLC. Our results highlight the potential of our MCA system for the detection of CTCs in patients with solid tumors such as lung cancer tumors and for further detailed molecular analyses of CTCs.

■ EXPERIMENTAL SECTION

Fabrication of CTC Enrichment Device. MCAs were made of nickel by electroforming as follows: a stainless steel plate was coated with SU-8 photoresists and exposed to UV light through a photomask to form the MCA pattern. By electroformation, nickel was built up in the bare areas of the stainless steel plate between the photoresists. Finally, the electroformed MCA was separated from the stainless steel plate. Each circular microcavity was fabricated with a diameter of 8−9 μm, and the rectangular microcavity was fabricated with a width of 5−9 μm and a length of 30 μm. The distance between each microcavity was 60 μm, and 10 000 (100 × 100) cavities were arranged in an 18 × 18 mm sheet (Figure 1a,b). A poly(dimethylsiloxane) (PDMS) structure equipped with a vacuum microchannel (i.d. 500 μm) was fitted directly beneath the MCA to apply negative pressure for CTC isolation, while a chamber for blood sample introduction was constructed on the upper side (Figure 1d). Master mold substrates comprising poly(methyl methacrylate) (PMMA) were prepared by a computer-aided modeling machine (PNC-300; Roland DG Corp., Shizuoka, Japan). PDMS layers were then fabricated by pouring a mixture of Sylgard 184 silicone elastomer (Dow Corning Asia Ltd., Tokyo, Japan) and curing agent (10:1) onto either the master molds or a blank wafer, followed by curing for at least 20 min at 85 °C. Upon curing, the PDMS substrates were carefully peeled off the molds. The CTC enrichment device was constructed by assembling the MCA and the PDMS layers using spacer tape in the same manner as previously described.[31] The sample inlet was connected to a reservoir, while the vacuum microchannel was connected to a peristaltic pump.

Cell Culture and Labeling. The SCLC cell lines NCI-H69 and NCI-H82 and the NSCLC cell lines NCI-H358 and NCI-H441 were cultured in RPMI 1640 medium containing 2 mM L-glutamine (Sigma-Aldrich, Irvine, UK), 10% (v/v) FBS (Invitrogen Corp., Carlsbad, CA), and 1% (v/v) penicillin/

streptomycin solution (Invitrogen Corp.) for 3–4 days at 37 °C in a humidified atmosphere containing 5% CO_2. Immediately before each experiment, confluent cells were trypsinized and resuspended in PBS.

To measure tumor cell size, the cell size distribution was measured using a CASY cell counter and Analyzer System (Model TTC; Schärfe System GmbH, Reutlingen, Germany). In the performance test, the tumor cells were labeled with CellTracker Red CMTPX (Molecular Probes, Eugene, OR), and labeling was achieved by incubating the cells with a tracking dye (5 μM) for 30 min. The cells were then pelleted by centrifugation (200*g* for 5 min); the supernatant was decanted, and the cells were washed twice with PBS to remove any excess dye. Finally, the cells were resuspended in PBS containing 2 mM EDTA and 0.5% BSA.

Blood Sample Preparation. Normal human blood samples were collected from healthy donors at the Tokyo University of Agriculture and Technology in accordance with Institutional Review Board procedures. Samples were collected in a collection tube with EDTA to prevent coagulation and used within 24 h. The clinical study was conducted at Shizuoka Cancer Center (UMIN clinical trial registry, number UMIN000005189), and patients with pathologically proven SCLC with radiological evident metastatic lesions were eligible for the study. The institutional review board at Shizuoka Cancer Center approved the study protocol, and all patients provided written informed consent. Peripheral blood samples were collected from 16 patients with histologically or cytologically confirmed metastatic SCLC. For each patient, 10–15 mL of blood was collected in EDTA tubes for CTC enumeration by the MCA system and processed within 2 h.

Tumor Cell Entrapment Operation. Blood samples or cell suspensions (1–5 mL) were added to the reservoir. Subsequently, negative pressure was applied to the cell suspension with a peristaltic pump connected to the vacuum line. The sample was passed through the microcavities at a flow rate of 200 μL/min for 0.5–10 min. To remove blood cells that remained on the array, PBS containing 2 mM EDTA and 0.5% BSA (2 mL) was then added to the reservoir and passed through the microcavities at a flow rate of 200 μL/min for 10 min.

Staining of Trapped Cells for the Identification of CTCs. Cell fixation solution and cell staining solution were introduced into the reservoir and passed through the microcavities with a peristaltic pump after washing. To stain the CTCs with an anticytokeratin antibody, the trapped cells were fixed by passing 400 μL of 1% PFA in PBS through the MCA at a flow rate of 20 μL/min for 20 min. After washing with 100 μL of PBS, the cells were subsequently treated with 200 μL of 0.2% Triton X-100 in PBS at a flow rate of 20 μL/min for 10 min. After permeabilization, the cells were treated with 3% BSA in PBS at a flow rate of 20 μL/min for 30 min. To identify CTCs and leukocytes, 600 μL of cell staining solution containing 1 μg/mL Hoechst 33342 (Molecular Probes, Invitrogen Corp.), a cocktail of antipan-cytokeratin antibodies (Alexa488-AE1/AE3 [1:100 dilution; eBioscience, San Diego, CA] and FITC-CK3-6H5 [1:60 dilution; Miltenyi Biotec, Auburn, CA]) and a PE-labeled anti-CD45 antibody [1:120 dilution; BD Biosciences, San Jose, CA]) was passed through the microcavities at a flow rate of 20 μL/min for 30 min. Finally, the array was washed with 1 mL of PBS containing 2 mM EDTA and 0.5% BSA to remove excess dye.

Identification and Enumeration of CTCs by Fluorescence Microscopy. After the tumor cells were recovered, an image of the entire cell array area was obtained using a fluorescence microscope (BX61; Olympus Corporation, Tokyo, Japan) integrated with a 10× objective lens and a computer-operated motorized stage, WU, NIBA, and WIG filter sets, a cooled digital camera (DP-70; Olympus Corporation), and Lumina Vision acquisition software (Mitani Corporation, Tokyo, Japan). In clinical trials, an entire image of the cell array area was obtained using a fluorescence microscope (Axio Imager Z1; Carl Zeiss, Oberkochen, Germany) integrated with a 10× or 20× objective lens and a computer-operated motorized stage, WU, FITC, and Texas Red filter sets, a digital camera (AxioCam HRc; Carl Zeiss), and AxioVision acquisition software (Carl Zeiss). Image analysis was then performed, and objects satisfying the predetermined criteria were counted. Fluorescence intensities and morphometric characteristics such as cell size, shape, and nuclear size were considered when performing CTC identification and nontumor cell exclusion; cells were characterized by a round to oval morphology and a visible nucleus (i.e., Hoechst-33342 positive), and those that were positive for cytokeratin and negative for CD45 were identified as CTCs (Supporting Information Figure S-1).

Measurement of Pressure Drop across the MCA. To measure the pressure drop across the MCA, disposable blood pressure transducers (ADInstruments, Colorado Springs, CO) were connected to the upstream and downstream lines of the CTC recovery device. A multichannel data-recording unit (PowerLab System; ADInstruments) was used for continuous pressure monitoring, and data was analyzed using LabChart software (ADInstruments).

Statistical Analysis. For comparison of the recovery rate of rectangular MCA (ϕ 8 μm) with the circular MCA (8 × 30 μm), 1000 cells of each of NCI-H69, NCI-H82, and NCI-H358 were spiked into 1 mL of whole blood of a healthy donor and then processed by the MCA assay in triplicate. Comparison of the average number of tumor cells and leukocytes recovered were carried out using unpaired, two-tailed Student's *t*-test. In the clinical test, the same blood samples were processed through the circular and rectangular MCAs side-by-side. Comparison of the number of CTCs and leukocytes recovered was carried out using a two-tailed Wilcoxon test. In addition, we tested the correlations between variables by calculating the Spearman's rank correlation coefficients. All statistical analyses were performed using GraphPad Prism software (GraphPad Software, San Diego, CA, USA). *P* values of less than 0.05 were considered significant.

RESULTS AND DISCUSSION

Pressure Drop via the MCA. In a previous study, we optimized the size of the circular MCA system to enable efficient recovery of tumor cells from human whole blood without clogging.[31] Our device successfully recovered more than 80% of the tumor cells spiked in 1 mL of whole human blood without pretreatment (e.g., density gradient centrifugation or erythrocyte lysis) when 8–9 μm diameter microcavities were used. However, 1000–3000 leukocytes were trapped on the MCA when 1 mL of whole blood was passed through the MCA. Because the diameter of the circular microcavity was smaller than the tumor cells and leukocytes, a number of microcavities were occupied by single cells after whole blood filtration. Therefore, the pressure gradient across the circular

MCA increased during blood filtration, and this increase might have caused the loss of small tumor cells through the cavities and damage to trapped cells.

In this study, a rectangular MCA was developed to improve the recovery of small tumor cells. The width of this rectangular microcavity was designed to be 5–9 μm for effective capture of CTCs based on typical tumor cell size. The length of the rectangular microcavity was designed to be 30 μm to prevent the occupation of microcavities by single cells and increase the porosity of the substrate; the lengths of rectangular microcavities were measured by microscopic observation. The widths were measured to be 4.7 ± 0.1, 6.0 ± 0.2, 7.2 ± 0.1, 8.3 ± 0.1, and 9.2 ± 0.4 μm.

First, the pressure drop during filtration was compared between the circular and rectangular MCAs. During PBS filtration using either MCA, the pressure drop was similar (0.3–0.4 kPa). In contrast, during filtration of an NCI-H441 cell suspension containing an excess number of cells compared to the number of microcavities, the pressure drop across the MCA increased as a function of cell number (Figure 2). The

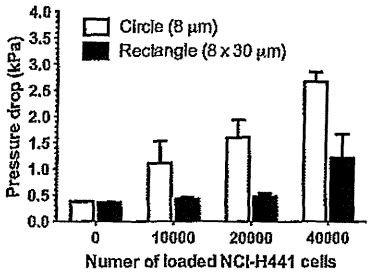

Figure 2. Pressure drop across the MCA during filtration of NCI-H441 cell suspensions.

pressure drop across the circular MCA was higher than that across the rectangular MCA due to occupation of microcavities by single cells. As shown in Figure 1c, although multiple cells were simultaneously trapped on single rectangular microcavities, the microcavities were not completely clogged.

The change in the pressure during filtration of a 3 mL whole blood sample and subsequent washing was then monitored (Figure 3). The pressure immediately increased after introduction of the blood sample and then gradually increased further as a function of filtration time. After washing solution was introduced, the pressure across the MCA immediately

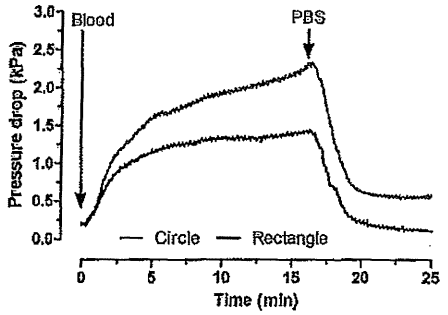

Figure 3. Monitoring the increase in pressure drop across the MCA during filtration of whole blood. Three milliliters of blood were introduced into the MCAs and then washed with PBS.

decreased. However, the maximum pressure drop across the circular MCA (2.3 kPa) was higher than that across the rectangular MCA (<1.5 kPa). In addition, with the rectangular MCA, the pressure returned to the original value after introduction of the washing buffer, whereas that of the circular MCA was slightly higher than the original value. This result suggests that some microcavities were occupied by blood cells with the circular MCA; the pressure was maintained at a higher level than the original value even after washing the MCA. These results suggest that the rectangular MCA enabled a reduction in the flow resistance and pressure drop across the microcavities in agreement with Kuo et al.[35]

Optimization of the Rectangular MCA. To optimize the design of the rectangular MCA, microcavities of various sizes were tested using tumor cell-spiked whole blood (Figure 4).

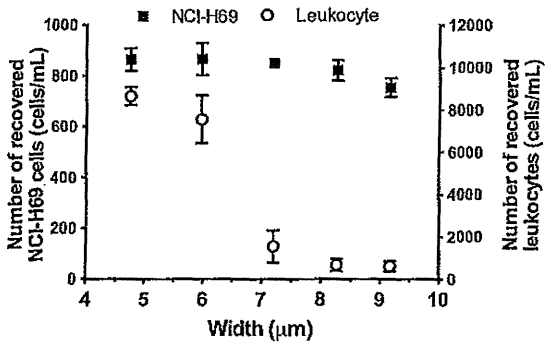

Figure 4. Relationship between the size of the rectangular microcavities and the number of recovered cells. Whole blood samples were spiked with CellTracker Red-stained NCI-H69 cells at 1000 cells/mL and recovered using various MCAs. The average number of tumor cells and leukocytes recovered is given.

The widths of the rectangular microcavities fabricated in this study were considerably smaller than the average diameter of the SCLC cell lines NCI-H69 (12.5 μm) and NCI-H82 (13.5 μm). Although the number of NCI-H69 cells recovered decreased slightly as the width of the rectangular microcavity increased, the recovery rates of all rectangular MCAs were higher than those of the circular MCAs. In addition, the number of trapped leukocytes varied according to the width of the rectangular microcavity. When the average width of the rectangular microcavity was greater than 7 μm, a number of leukocytes passed through the microcavities, resulting in a decrease in the number of captured leukocytes. Our previous study showed that the number of leukocytes captured depended on the effects of size, i.e., the size difference between leukocytes and microcavities, and retention, i.e., cellular deformability and adhesiveness.[30] Since leukocytes include cells that differ in size, deformability, and adhesiveness, the number of captured cells increased as the width of the MCA decreased. Therefore, to obtain a high recovery rate and high tumor cell purity, subsequent tumor cell-recovery experiments were conducted using rectangular MCAs containing microcavities with an average width of 8 μm.

To compare the recovery rates of the rectangular and circular MCAs, an NSCLC cell line (NCI-H358) and 2 SCLC cell lines (NCI-H69 and NCI-H82) were evaluated. When NCI-H358 cells were used in the recovery test, no obvious difference was observed between the 2 MCAs (Table 1). In contrast, when NCI-H69 and NCI-H82 cells were used, the recovery rates

dx.doi.org/10.1021/ac400167x | Anal. Chem. 2013, 85, 5692–5698

Table 1. Comparison of the Cell Recovery Rates between the Circular and Rectangular MCAs[a]

	number of recovered cells			
microcavity type	NCI-H358	NCI-H69	NCI-H82	leukocytes
circular	897 ± 40	672 ± 75	646 ± 58	1515 ± 334
rectangular	898 ± 34	802 ± 48	829 ± 49	251 ± 30

[a]Whole blood samples were spiked with 3 different lung cancer cell lines, NCI-H358, NCI-H69, and NCI-H82, at 1000 cells/mL and were recovered using the circular MCA (ϕ 8 μm) and the rectangular MCA (8 × 30 μm). The average number of tumor cells and leukocytes recovered is shown.

using the optimized rectangular MCA (80% ± 5% and 83% ± 5%, respectively) were significantly higher than those using the circular MCA (67% ± 7%; $p = 0.01$ by t-test and 65 ± 6%; $p < 0.01$ by t-test, respectively). In addition, the number of leukocytes captured on the rectangular MCA was 7-fold lower than that captured on the circular MCA. As a result, tumor cells were enriched more than 7000-fold on the rectangular MCA from whole blood. As described above, the occupation of microcavities by blood cells increased the pressure. We observed that, once cells occupied the circular microcavities, other cells were preferentially driven toward the unoccupied microcavities and passed through them at a higher pressure. Therefore, we believe that the excessive flow resistance and pressure increase caused cell deformation and allowed the cells to pass through the circular microcavities, resulting in increased loss of small tumor cells such as SCLC cells. The fluctuation in pressure during filtration using the rectangular MCA was smaller than that using the circular MCA. The rectangular MCA enabled recovery of small tumor cells with high efficiency.

We previously reported that approximately 98% of cells recovered with the circular MCA were viable.[31] In this study, the viability of the recovered tumor cells was further validated by expanding the cells in culture. NCI-H358 cells recovered on the MCA were retrieved with a micropipet and then reseeded in a culture dish. Adherence and growth of the NCI-H358 cells captured from whole blood was observed (Supporting Information Figure S-2).

Study of Blood Sample Preparation. This study was aimed at understanding the conditions that enable efficient direct recovery of small tumor cells from whole blood. Small-sized tumor cells and cellular aggregates can be lost as a result of blood sample pretreatments before filtration, such as density gradient centrifugation and erythrocyte lysis, because they require a cycle of decantation and pipetting, resulting in the loss of rare cells. In addition, due to either the migration of cells to the plasma layer or the presence of aggregates, CTCs can be easily lost during density gradient centrifugation.[36] In addition, we avoided cell fixation before filtration to recover intact CTCs. To evaluate the effect of anticoagulants on blood filtration, heparin tubes were also used for blood collection and spiked tumor cell recoveries were compared. During filtration of 1 mL of whole blood collected in a heparin tube, the pressure across the circular and rectangular MCAs increased by 40 and 9.5 kPa, respectively, suggesting that the microcavities were clogged by blood cells. Indeed, fluorescent imaging of the array after filtration of whole blood collected in a heparin tube showed blood clotting (data not shown). Therefore, all experiments were performed using blood collected in an EDTA tube, and the effect of the time that elapsed before mixing the collected blood with anticoagulant on the recovery of spiked tumor cells was determined. Blood was collected without using an anticoagulant and then dispensed into EDTA tubes after a certain period; as a result, the recovery rates of spiked tumor cells varied according to the time that elapsed before mixing the collected blood with an anticoagulant (Supporting Information Figure S-3). The cell recovery of a sample prepared 1 min after blood collection was approximately 10% lower than that of a sample prepared immediately after blood collection. This was confirmed by clogging of the array in the fluorescence images after filtration of these samples. Furthermore, the number of macroscopic blood clots on the array was increased as a function of elapsed time. Therefore, we collected blood samples

Table 2. Numbers of CTCs and Leukocytes Recovered from SCLC Patients Using the Circular and the Rectangular MCAs

	number of recovered CTCs (cells/mL)		number of recovered leukocytes (cells/mL)		percentage of CTCs in total captured cells (%)	
patient no.	circular MCA	rectangular MCA	circular MCA	rectangular MCA	circular MCA	rectangular MCA
1	1.7	2.3	2677	456	0.06	0.51
2	1.3	11.3	3741	2569	0.03	0.44
3	5.3	51.3	4354	4652	0.12	1.09
4	0.9	3.0	1556	545	0.06	0.55
5	3.0	2.0	1831	881	0.16	0.23
6	1.8	4.5	2843	1516	0.06	0.29
7	16.3	12.6	2096	1096	0.77	1.13
8	0.3	14.7	2613	3188	0.01	0.46
9	1.7	1.4	2781	457	0.06	0.31
10	0.6	0.9	3611	660	0.02	0.14
11	5.3	2.1	2058	598	0.26	0.34
12	4.9	0.3	2197	855	0.22	0.03
13	14.7	0.6	2014	852	0.72	0.07
14	0.3	0.7	1460	630	0.02	0.11
15	3.0	0.4	1063	659	0.28	0.06
16	19.3	72.7	2341	2605	0.82	2.71
median ± SEM	2.4 ± 1.5	2.2 ± 5.2	2269 ± 220	854 ± 306	0.09 ± 0.07	0.33 ± 0.17

dx.doi.org/10.1021/ac400167x | Anal. Chem. 2013, 85, 5692−5698

using evacuated blood collection tubes to prevent blood coagulation.

Clinical Test. For the clinical evaluation, 16 patients with extensive SCLC were enrolled in the study. The same blood samples were processed through the circular and rectangular MCAs side-by-side. Joosse et al. reported that broadening the spectrum of keratin detection increased CTC detection, thereby reducing the number of false-negatives.[37] Therefore, in this study, to stain a broad range of keratins, an anticytokeratin antibody cocktail of Alexa488-AE1/AE3 and FITC-CK3-6H5 was used for CTC detection. In addition, to evaluate the detection sensitivity and capacity, 7.5 mL of healthy donor blood, spiked with 1 tumor cell, was assessed with the MCA used in the recent report.[32] Therefore, we believe that the capacity of this method is limited to 7.5 mL of whole blood. In this study, we performed the clinical tests with 2–4 mL of whole blood considering the heterogeneity of patients' blood samples.

With the rectangular MCA, CTCs were detectable in 16 of 16 SCLC patients (Table 2). The number of CTCs isolated with the rectangular (range, 0.3–72.7 cells/mL; median, 2.2 cells/mL) and circular MCAs (range, 0.3–19.3 cells/mL; median, 2.4 cells/mL) did not differ significantly (p = 0.60, Wilcoxon test).[32] There was no statistically significant correlation between them (Spearman's rho was 0.14, p = 0.60). We speculated that the reason for this was the tendency of circulating CTCs in clinical samples to form aggregates, including CTC clusters that are large enough to be captured on single microcavities. In contrast, the number of leukocytes captured with the rectangular (range, 456–4652 cells/mL; median, 854 cells/mL) and circular MCAs (range, 1063–4354 cells/mL; median, 2269 cells/mL) differed significantly (p < 0.001, Wilcoxon test). There was no statistically significant correlation between them (Spearman's rho was 0.41, p = 0.12). The percentage of CTCs in total captured cells on the rectangular MCA (0.33% ± 0.17%) was significantly higher that on the circular MCA (0.09% ± 0.07%) (p = 0.03, Wilcoxon test). There was no statistically significant correlation between them (Spearman's rho was 0.09, p = 0.73). On average, the number of leukocytes captured with the rectangular MCA was approximately 2-fold lower than that with the circular MCA. However, the number of leukocytes captured varied widely among patients compared to the number of leukocytes from normal blood samples. We attributed this to the differences between cancer patients and normal volunteers in blood properties, such as viscosity and aggregability, which depend on plasma protein concentration or hematocrit. Although we have improved the number and purity of small tumor cells recovered from whole blood in this study (which might be lost with the conventional size-based enrichment methods), further clinical studies should be performed with larger cohorts of patients with various types of cancers to improve the number and purity of CTCs isolated from patient blood. In previous reports,[31,32] we performed the CTC enumeration assays using negative control samples (healthy donor blood). In these samples, no CTCs (false-positive) were observed by fluorescent imaging. However, leukocytes clogged the microcavities, increasing the background fluorescent noise of the MCA substrate or trapped cells. Therefore, we believe that the reduction in the number of leukocytes captured on the MCA is a significant factor for the prevention of false-positive CTCs and further gene analysis of CTCs.

Recently, various microfluidic devices have been developed to improve the enrichment of CTCs from whole blood.[24,27,28,35,38] The advantage of the size-based enrichment techniques is that it enables simple and rapid processing of a large volume of whole blood (≥1 mL) compared to other techniques. In addition, our microcavity array was integrated with a microfluidic device so that enrichment, staining, and washing processes in the microfluidic assay could be performed within one integrated device. We have also developed a technique for single cell isolation by using microcapillaries and subsequent gene analysis using MCA.[29,39] We could obtain only CTCs from a patients' blood by integrating these techniques with the rectangular MCA. However, further clinical studies should be performed with larger cohorts of patients with various types of cancers to assess whether the MCA system is a more appropriate tool for CTC enumeration and characterization of metastatic tumors in patients with cancers other than lung cancer.

CONCLUSION

In this study, we improved the structure of the MCA to efficiently recover small-sized tumor cells by size-based isolation of tumor cells from whole blood. Using this system, CTCs were successfully recovered from the whole blood of patients with SCLC with higher purity than the previously developed system. Therefore, the MCA system has potential as a tool for the efficient recovery of CTCs with high purity in patients with small cell-type tumors, while offering additional advantages in cost, portability, and capacity for further detailed analyses of CTCs.

ASSOCIATED CONTENT

Supporting Information

Additional information as noted in text. This material is available free of charge via the Internet at http://pubs.acs.org.

AUTHOR INFORMATION

Corresponding Author

*Fax: +81-42-385-7713. Phone: +81-42-388-7020. E-mail: tmatsuna@cc.tuat.ac.jp.

Notes

The authors declare the following competing financial interest(s): MH, TYoshino, YKikuhara, HKanbara, and TM have applied for patents related to the MCA system.

ACKNOWLEDGMENTS

This work was partly supported by Regional Innovation Cluster Program and a Grant-in-Aid for Research Fellowship for Young Scientists (11J11150) from the Ministry of Education, Culture, Sports, Science and Technology of Japan.

REFERENCES

(1) Riethdorf, S.; Pantel, K. *Ann. N.Y. Acad. Sci.* **2010**, *1210*, 66–77.

(2) Cristofanilli, M.; Hayes, D. F.; Budd, G. T.; Ellis, M. J.; Stopeck, A.; Reuben, J. M.; Doyle, G. V.; Matera, J.; Allard, W. J.; Miller, M. C.; Fritsche, H. A.; Hortobagyi, G. N.; Terstappen, L. W. *J. Clin. Oncol.* **2005**, *23* (7), 1420–1430.

(3) Pestrin, M.; Bessi, S.; Galardi, F.; Truglia, M.; Biggeri, A.; Biagioni, C.; Cappadona, S.; Biganzoli, L.; Giannini, A.; Di Leo, A. *Breast Cancer Res. Treat.* **2009**, *118* (3), 523–530.

(4) Fehm, T.; Muller, V.; Aktas, B.; Janni, W.; Schneeweiss, A.; Stickeler, E.; Lattrich, C.; Lohberg, C. R.; Solomayer, E.; Rack, B.; Riethdorf, S.; Klein, C.; Schindlbeck, C.; Brocker, K.; Kasimir-Bauer,

S.; Wallwiener, D.; Pantel, K. *Breast Cancer Res. Treat.* 2010, *124* (2), 403–412.
(5) Maheswaran, S.; Sequist, L. V.; Nagrath, S.; Ulkus, L.; Brannigan, B.; Collura, C. V.; Inserra, E.; Diederichs, S.; Iafrate, A. J.; Bell, D. W.; Digumarthy, S.; Muzikansky, A.; Irimia, D.; Settleman, J.; Tompkins, R. G.; Lynch, T. J.; Toner, M.; Haber, D. A. *N. Engl. J. Med.* 2008, *359* (4), 366–377.
(6) Stott, S. L.; Hsu, C. H.; Tsukrov, D. I.; Yu, M.; Miyamoto, D. T.; Waltman, B. A.; Rothenberg, S. M.; Shah, A. M.; Smas, M. B.; Korir, G. K.; Floyd, F. P., Jr.; Gilman, A. J.; Lord, J. B.; Winokur, D.; Springer, S.; Irimia, D.; Nagrath, S.; Sequist, L. V.; Lee, R. J.; Isselbacher, K. J.; Maheswaran, S.; Haber, D. A.; Toner, M. *Proc. Natl. Acad. Sci. U. S. A.* 2010, *107* (43), 18392–18397.
(7) Riethdorf, S.; Fritsche, H.; Muller, V.; Rau, T.; Schindlbeck, C.; Rack, B.; Janni, W.; Coith, C.; Beck, K.; Janicke, F.; Jackson, S.; Gornet, T.; Cristofanilli, M.; Pantel, K. *Clin. Cancer Res.* 2007, *13* (3), 920–928.
(8) Allard, W. J.; Matera, J.; Miller, M. C.; Repollet, M.; Connelly, M. C.; Rao, C.; Tibbe, A. G.; Uhr, J. W.; Terstappen, L. W. *Clin. Cancer Res.* 2004, *10* (20), 6897–6904.
(9) Sieuwerts, A. M.; Kraan, J.; Bolt, J.; van der Spoel, P.; Elstrodt, F.; Schutte, M.; Martens, J. W.; Gratama, J. W.; Sleijfer, S.; Foekens, J. A. *J. Natl. Cancer Inst.* 2009, *101* (1), 61–66.
(10) Went, P. T.; Lugli, A.; Meier, S.; Bundi, M.; Mirlacher, M.; Sauter, G.; Dirnhofer, S. *Hum. Pathol.* 2004, *35* (1), 122–128.
(11) Paterlini-Brechot, P.; Benali, N. L. *Cancer Lett.* 2007, *253* (2), 180–204.
(12) Mikolajczyk, S. D.; Millar, L. S.; Tsinberg, P.; Coutts, S. M.; Zomorrodi, M.; Pham, T.; Bischoff, F. Z.; Pircher, T. J. *J. Oncol.* 2011, *2011*, 252361.
(13) Raimondi, C.; Gradilone, A.; Naso, G.; Vincenzi, B.; Petracca, A.; Nicolazzo, C.; Palazzo, A.; Saltarelli, R.; Spremberg, F.; Cortesi, E.; Gazzaniga, P. *Breast Cancer Res. Treat.* 2011, *130* (2), 449–455.
(14) Pecot, C. V.; Bischoff, F. Z.; Mayer, J. A.; Wong, K. L.; Pham, T.; Bottsford-Miller, J.; Stone, R. L.; Lin, Y. G.; Jaladurgam, P.; Roh, J. W.; Goodman, B. W.; Merritt, W. M.; Pircher, T. J.; Mikolajczyk, S. D.; Nick, A. M.; Celestino, J.; Eng, C.; Ellis, L. M.; Deavers, M. T.; Sood, A. K. *Cancer Discovery* 2011, *1* (7), 580–586.
(15) Krebs, M. G.; Hou, J. M.; Sloane, R.; Lancashire, L.; Priest, L.; Nonaka, D.; Ward, T. H.; Backen, A.; Clack, G.; Hughes, A.; Ranson, M.; Blackhall, F. H.; Dive, C. *J. Thorac. Oncol.* 2012, *7* (2), 306–315.
(16) Vona, G.; Estepa, L.; Beroud, C.; Damotte, D.; Capron, F.; Nalpas, B.; Mineur, A.; Franco, D.; Lacour, B.; Pol, S.; Brechot, C.; Paterlini-Brechot, P. *Hepatology* 2004, *39* (3), 792–797.
(17) Vona, G.; Sabile, A.; Louha, M.; Sitruk, V.; Romana, S.; Schutze, K.; Capron, F.; Franco, D.; Pazzagli, M.; Vekemans, M.; Lacour, B.; Brechot, C.; Paterlini-Brechot, P. *Am. J. Pathol.* 2000, *156* (1), 57–63.
(18) Zabaglo, L.; Ormerod, M. G.; Parton, M.; Ring, A.; Smith, I. E.; Dowsett, M. *Cytometry, Part A* 2003, *55* (2), 102–108.
(19) Desitter, I.; Guerrouahen, B. S.; Benali-Furet, N.; Wechsler, J.; Janne, P. A.; Kuang, Y.; Yanagita, M.; Wang, L.; Berkowitz, J. A.; Distel, R. J.; Cayre, Y. E. *Anticancer Res.* 2011, *31* (2), 427–441.
(20) Farace, F.; Massard, C.; Vimond, N.; Drusch, F.; Jacques, N.; Billiot, F.; Laplanche, A.; Chauchereau, A.; Lacroix, L.; Planchard, D.; Le Moulec, S.; Andre, F.; Fizazi, K.; Soria, J. C.; Vielh, P. *Br. J. Cancer* 2011, *105* (6), 847–853.
(21) Hou, J. M.; Krebs, M.; Ward, T.; Sloane, R.; Priest, L.; Hughes, A.; Clack, G.; Ranson, M.; Blackhall, F.; Dive, C. *Am. J. Pathol.* 2011, *178* (3), 989–996.
(22) Hofman, V.; Ilie, M. I.; Long, E.; Selva, E.; Bonnetaud, C.; Molina, T.; Venissac, N.; Mouroux, J.; Vielh, P.; Hofman, P. *Int. J. Cancer* 2011, *129* (7), 1651–1660.
(23) Bhagat, A. A.; Hou, H. W.; Li, L. D.; Lim, C. T.; Han, J. *Lab Chip* 2011, *11* (11), 1870–1878.
(24) McFaul, S. M.; Lin, B. K.; Ma, H. *Lab Chip* 2012, *12* (13), 2369–2376.
(25) Tan, S. J.; Lakshmi, R. L.; Chen, P.; Lim, W. T.; Yobas, L.; Lim, C. T. *Biosens. Bioelectron.* 2010, *26* (4), 1701–1705.
(26) Zheng, S.; Lin, H. K.; Lu, B.; Williams, A.; Datar, R.; Cote, R. J.; Tai, Y. C. *Biomed. Microdevices* 2011, *13* (1), 203–213.
(27) Park, J. M.; Lee, J. Y.; Lee, J. G.; Jeong, H.; Oh, J. M.; Kim, Y. J.; Park, D.; Kim, M. S.; Lee, H. J.; Oh, J. H.; Lee, S. S.; Lee, W. Y.; Huh, N. *Anal. Chem.* 2012, *84* (17), 7400–7407.
(28) Lim, L. S.; Hu, M.; Huang, M. C.; Cheong, W. C.; Gan, A. T.; Looi, X. L.; Leong, S. M.; Koay, E. S.; Li, M. H. *Lab Chip* 2012, *12* (21), 4388–4396.
(29) Hosokawa, M.; Arakaki, A.; Takahashi, M.; Mori, T.; Takeyama, H.; Matsunaga, T. *Anal. Chem.* 2009, *81* (13), 5308–5313.
(30) Hosokawa, M.; Asami, M.; Nakamura, S.; Yoshino, T.; Tsujimura, N.; Takahashi, M.; Nakasono, S.; Tanaka, T.; Matsunaga, T. *Biotechnol. Bioeng.* 2012, *109* (8), 2017–2024.
(31) Hosokawa, M.; Hayata, T.; Fukuda, Y.; Arakaki, A.; Yoshino, T.; Tanaka, T.; Matsunaga, T. *Anal. Chem.* 2010, *82* (15), 6629–6635.
(32) Hosokawa, M.; Kenmotsu, H.; Koh, Y.; Yoshino, T.; Tanaka, T.; Yoshikawa, T.; Naito, T.; Takahashi, T.; Murakami, H.; Nakamura, Y.; Tsuya, A.; Shukuya, T.; Ono, A.; Akamatsu, H.; Watanabe, R.; Ono, S.; Mori, K.; Kanbara, H.; Yamaguchi, K.; Matsunaga, T.; Yamamoto, N. *PLoS One* 2013, DOI: 10.1371/journal.pone.0067466.
(33) Marrinucci, D.; Bethel, K.; Bruce, R. H.; Curry, D. N.; Hsieh, B.; Humphrey, M.; Krivacic, R. T.; Kroener, J.; Kroener, L.; Ladanyi, A.; Lazarus, N. H.; Nieva, J.; Kuhn, P. *Hum. Pathol.* 2007, *38* (3), 514–519.
(34) Marrinucci, D.; Bethel, K.; Lazar, D.; Fisher, J.; Huynh, E.; Clark, P.; Bruce, R.; Nieva, J.; Kuhn, P. *J. Oncol.* 2010, *2010*, 861341.
(35) Kuo, J. S.; Zhao, Y.; Schiro, P. G.; Ng, L.; Lim, D. S.; Shelby, J. P.; Chiu, D. T. *Lab Chip* 2010, *10* (7), 837–842.
(36) Alunni-Fabbroni, M.; Sandri, M. T. *Methods* 2010, *50* (4), 289–297.
(37) Joosse, S. A.; Hannemann, J.; Spotter, J.; Bauche, A.; Andreas, A.; Muller, V.; Pantel, K. *Clin. Cancer Res.* 2012, *18* (4), 993–1003.
(38) Chen, W.; Weng, S.; Zhang, F.; Allen, S.; Li, X.; Bao, L.; Lam, R. H.; Macoska, J. A.; Merajver, S. D.; Fu, J. *ACS Nano* 2013, *7* (1), 566–575.
(39) Arakaki, A.; Ooya, K.; Akiyama, Y.; Hosokawa, M.; Komiyama, M.; Iizuka, A.; Yamaguchi, K.; Matsunaga, T. *Biotechnol. Bioeng.* 2010, *106* (2), 311–318.

PLOS ONE

Size-Based Isolation of Circulating Tumor Cells in Lung Cancer Patients Using a Microcavity Array System

Masahito Hosokawa[1,2], Hirotsugu Kenmotsu[3], Yasuhiro Koh[2], Tomoko Yoshino[1], Takayuki Yoshikawa[1], Tateaki Naito[3], Toshiaki Takahashi[3], Haruyasu Murakami[3], Yukiko Nakamura[3], Asuka Tsuya[3], Takehito Shukuya[3], Akira Ono[3], Hiroaki Akamatsu[3], Reiko Watanabe[4], Sachiyo Ono[4], Keita Mori[5], Hisashige Kanbara[6], Ken Yamaguchi[2], Tsuyoshi Tanaka[1], Tadashi Matsunaga[1], Nobuyuki Yamamoto[3]*

1 Division of Biotechnology and Life Science, Institute of Engineering, Tokyo University of Agriculture and Technology, Tokyo, Japan, **2** Drug Discovery and Development Division, Shizuoka Cancer Center Research Institute, Shizuoka, Japan, **3** Division of Thoracic Oncology, Shizuoka Cancer Center, Shizuoka, Japan, **4** Division of Diagnostic Pathology, Shizuoka Cancer Center, Shizuoka, Japan, **5** Clinical Trial Coordination Office, Shizuoka Cancer Center, Shizuoka, Japan, **6** Hitachi Chemical Co., Ltd., Tokyo, Japan

Abstract

Background: Epithelial cell adhesion molecule (EpCAM)-based enumeration of circulating tumor cells (CTC) has prognostic value in patients with solid tumors, such as advanced breast, colon, and prostate cancer. However, poor sensitivity has been reported for non-small cell lung cancer (NSCLC). To address this problem, we developed a microcavity array (MCA) system integrated with a miniaturized device for CTC isolation without relying on EpCAM expression. Here, we report the results of a clinical study on CTCs of advanced lung cancer patients in which we compared the MCA system with the CellSearch system, which employs the conventional EpCAM-based method.

Methods: Paired peripheral blood samples were collected from 43 metastatic lung cancer patients to enumerate CTCs using the CellSearch system according to the manufacturer's protocol and the MCA system by immunolabeling and cytomorphological analysis. The presence of CTCs was assessed blindly and independently by both systems.

Results: CTCs were detected in 17 of 22 NSCLC patients using the MCA system versus 7 of 22 patients using the CellSearch system. On the other hand, CTCs were detected in 20 of 21 small cell lung cancer (SCLC) patients using the MCA system versus 12 of 21 patients using the CellSearch system. Significantly more CTCs in NSCLC patients were detected by the MCA system (median 13, range 0–291 cells/7.5 mL) than by the CellSearch system (median 0, range 0–37 cells/7.5 ml) demonstrating statistical superiority ($p = 0.0015$). Statistical significance was not reached in SCLC though the trend favoring the MCA system over the CellSearch system was observed ($p = 0.2888$). The MCA system also isolated CTC clusters from patients who had been identified as CTC negative using the CellSearch system.

Conclusions: The MCA system has a potential to isolate significantly more CTCs and CTC clusters in advanced lung cancer patients compared to the CellSearch system.

Citation: Hosokawa M, Kenmotsu H, Koh Y, Yoshino T, Yoshikawa T, et al. (2013) Size-Based Isolation of Circulating Tumor Cells in Lung Cancer Patients Using a Microcavity Array System. PLoS ONE 8(6): e67466. doi:10.1371/journal.pone.0067466

Editor: William C S Cho, Queen Elizabeth Hospital, Hong Kong

Received January 18, 2013; **Accepted** May 17, 2013; **Published** June 28, 2013

Funding: This work was partly supported by the Regional Innovation Cluster Program and a Grant-in-Aid for Research Fellowship for Young Scientists (11J11150) from the Ministry of Education, Culture, Sports, Science and Technology of Japan. The funders had no role in study design, data collection and analysis, decision to publish, or preparation of the manuscript.

Competing Interests: MH, TYoshino, HKanbara, and TM have applied for patents related to the MCA system. HKanbara is employed by Hitachi Chemical Co., Ltd. This does not alter the authors' adherence to all the PLOS ONE policies on sharing data and materials.

* E-mail: n.yamamoto@scchr.jp

Introduction

Lung cancer is the leading cause of cancer-related death in most industrialized countries. Small cell lung cancer (SCLC) accounts for approximately 15% of lung cancer cases, and non-small cell lung cancer (NSCLC), which includes adenocarcinoma (ADC) and squamous cell carcinoma (SCC), accounts for 85% of lung cancer cases. It has recently been shown that identification of NSCLC patients by detection of genetic aberrations, specifically *EGFR*-activating mutations and the *EML4-ALK* fusion gene, allows for better prediction of response to EGFR tyrosine kinase inhibitors and ALK inhibitors, respectively [1,2]. Despite advances in prevention and treatment, NSCLC patients are often diagnosed at an advanced stage and have a poor prognosis due to the disease's tendency toward distant metastasis, the primary cause of mortality among NSCLC patients. Characterized by aggressive tumor growth and often presenting with metastases in the regional nodes and distant organs, SCLC is initially highly sensitive to chemotherapy but tends to acquire chemoresistance, leading to inevitable relapse.

Circulating tumor cells (CTCs) are defined as tumor cells circulating in the peripheral blood of patients with metastatic cancer. When measured using the US Food and Drug Adminis-

tration (FDA)-approved CellSearch system (Veridex, Raritan, NJ, USA), the number of CTCs in peripheral blood can be used to predict the prognosis of patients with metastatic breast cancer [3], colorectal cancer [4], prostate cancer [5], NSCLC [6], and SCLC [7]. The CellSearch system enriches CTCs using magnetic beads coated with a monoclonal antibody-targeting epithelial cell marker, such as the epithelial cell-adhesion molecule (EpCAM) [8,9]. However, several studies have shown that the presence of EpCAM on tumor cells varies with tumor type [10,11]. The expression of epithelial cell markers, including EpCAM, is downregulated to increase invasiveness and metastatic potential by epithelial-to-mesenchymal transition (EMT) [12–16]. It has been suggested that the low prevalence of CTCs detected in patients with advanced NSCLC using the CellSearch system may be due to the loss of EpCAM expression [17], indicating that EpCAM-based CTC isolation methods cannot achieve stable and reproducible CTC recovery from all tumor types.

Other CTC isolation methods are mainly based on differences in the size and deformability between CTCs and hematologic cells. As tumor cells (>8 μm) are larger than leukocytes [18–21], isolation by size of epithelial tumor cells (ISET) can be achieved using filtration to separate individual cells. ISET using a polycarbonate filter, an inexpensive, user-friendly method of enriching CTCs, enables the recovery and detection of epithelial-marker-negative CTCs on the basis of size-dependent CTC isolation. In clinical tests, use of an ISET-based system has been found to achieve higher CTC detection sensitivity in patients with metastatic lung cancer compared to use of the CellSearch system [22–24].

Recently, microfabricated devices for size-based separation of tumor cells have been widely developed to enable precise and efficient enrichment of CTCs from whole blood [25–28]. These devices include a miniaturized microcavity array (MCA) system that we developed for the highly efficient entrapment of single cells by filtration based on differences in the sizes of cells [29,30]. In a previous study, we examined the application of our MCA system to the detection of spiked tumor cells from unprocessed human whole blood based on differences in the size and deformability between tumor cells and other blood cells [31]. Using our device, we were able to entrap tumor cells onto size- and geometry-controlled microcavity arrays composed of 10,000 apertures by applying negative pressure, allowing the entrapped cells to be easily enumerated and analyzed by microscopic imaging of specified areas. Furthermore, we found that use of the miniaturized device allowed for introduction of a series of reagents for detection of tumor cells through the microfluidic structure. Our results indicate that our system is a simple yet precise system for the detection of tumor cells within whole blood. To confirm and build on our previous findings, we compared the capacity and efficiency of our novel MCA system and the current gold standard CellSearch system in performing CTC detection and enumeration in whole blood samples drawn from a cohort of NSCLC and SCLC patients.

Materials and Methods

Study Design and Ethics Statement

This prospective study was conducted to evaluate CTC enumeration using the CellSearch system and the MCA system in patients with metastatic lung cancer in a blinded experiment (UMIN clinical trial registry, number UMIN000005189). The presence of CTCs was assessed individually according to their criteria before knowing any results from each other. The study inclusion criteria were diagnosis of pathologically proven lung cancer with radiologically evident metastatic lesions, i.e., histologically or cytologically confirmed metastatic NSCLC or SCLC, and enrollment at the Shizuoka Cancer Center. The institutional review boards of the Shizuoka Cancer Center approved the study protocol, and all patients provided written informed consent. From each of the 43 patients who were enrolled, among whom 22 had been diagnosed with NSCLC and 21 with SCLC, 10–15 mL of blood was collected in EDTA tubes for CTC enumeration by the MCA system in our laboratory (Shizuoka Cancer Center, Shizuoka, Japan) and 20 mL was collected in CellSave collection tubes for CTC enumeration by the CellSearch system in the laboratory of SRL Inc. (Tokyo, Japan).

Cell Culture and Labeling

HCC827, NCI-H358, NCI-H441, DMS79, NCI-H69, and NCI-H82 cell lines were purchased from the American Type Culture Collection without further testing or authentication. A549 (Riken Bioresource Center, Tsukuba, Japan) and PC-14 [32] were kindly provided by Dr. Fumiaki Koizumi (National Cancer Center, Tokyo, Japan). The A549, HCC827, NCI-H358, NCI-H441, PC-14, DMS79, NCI-H69, and NCI-H82 NSCLC and SCLC cell lines were cultured in RPMI 1640 medium containing 2 mM of L-glutamine (Sigma-Aldrich, Irvine, UK), 10% (v/v) fetal bovine serum (FBS; Invitrogen Corp., Carlsbad, CA, USA), and 1% (v/v) penicillin/streptomycin (Invitrogen Corp.) for 3–4 days at 37°C with 5% CO_2 supplementation. Immediately prior to each experiment, cells grown to confluence were trypsinized and resuspended in phosphate-buffered saline (PBS). As a measurement of tumor cell size, cell size distribution was determined using the CASY® Cell Counter+Analyzer System Model TTC (Schärfe System GmbH, Reutlingen, Germany). To evaluate device performance, the tumor cell lines were labeled with CellTracker Red CMTPX (Molecular Probes, Eugene, OR, USA), with labeling achieved by incubating the cells with a tracking dye (5 μM) for 30 min. After the cells had been pelleted by centrifugation (200 g for 5 min), the supernatant was decanted. The cells were then washed twice with PBS to remove any excess dye before being resuspended in PBS containing 2 mM EDTA and 0.5% bovine serum albumin (BSA).

Fabrication of the MCA System

The MCA system was fabricated in the same manner as previously reported [29,31]. For CTC enumeration with fluorescence microscope observation, an MCA that had been manufactured by electroforming of nickel was used. For CTC morphological analysis by Giemsa staining, a transparent MCA that had been manufactured by laser irradiation of poly(ethylene terephthalate) (PET) was used. Each of the 10,000 cavities arranged in each 100×100 array was fabricated to have a diameter of 8–9 μm at the top surface and to be 60 μm distant from the adjacent microcavity. Poly(dimethylsiloxane) (PDMS) structures were fabricated and then integrated with the MCA such that the upper substrate consisted of a microchamber, a sample inlet, and an outlet, while the lower substrate beneath the MCA contained a vacuum line to produce negative pressure, enabling cell entrapment. The CTC isolation device was constructed by assembling the MCA, while the upper and lower PDMS layers were constructed using spacer tapes (Figure 1a). The sample inlet was connected to a reservoir, while the vacuum microchannel was connected to a peristaltic pump.

CTC Enumeration using the MCA System

Human blood samples were collected in a collection tube with EDTA to prevent coagulation and used within 2 h. The average

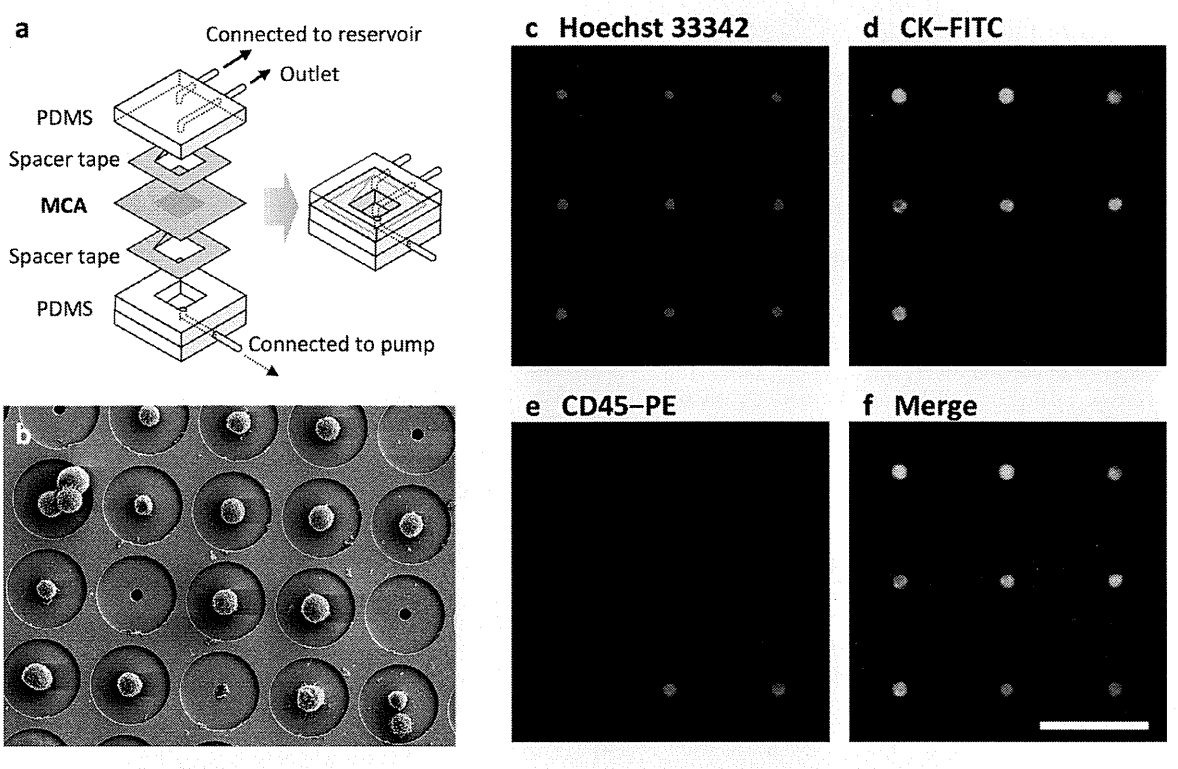

Figure 1. MCA system for size-based isolation of CTCs. (a) Schematic diagram of the structure of the MCA system. (b) Scanning electron microscope image of a cultured tumor cell line trapped on the MCA system. (c–f) Cells isolated from SCLC patient blood stained with Hoechst 33342 (c) and fluorescent-labeled antibodies that target cytokeratin (d) and CD45 (e). Merging of the images (f) allowed for identification of CTCs and hematologic cells. Scale bar = 60 μm.
doi:10.1371/journal.pone.0067466.g001

volume of blood analyzed was 4.0 mL per sample (range, 3.0–7.5 mL). All CTC enumeration using the MCA system was performed without knowledge of patient clinical status in the laboratory of the Shizuoka Cancer Center Research Institute. After introduction of blood samples into the reservoir, negative pressure was applied to a cell suspension using a peristaltic pump connected to a vacuum line, allowing the sample to be passed through the microcavities at a flow rate of 200 μL/min. To remove any blood cells remaining on the array, PBS containing 2 mM EDTA and 0.5% BSA (1 mL) was introduced into the reservoir and passed through the microcavities at a flow rate of 200 μL/min for 5 min.

To stain the CTCs with anti-pancytokeratin antibody, trapped cells were fixed by flowing 400 μL of 1% paraformaldehyde (PFA) in PBS through the MCA at a flow rate of 20 μL/min for 20 min. After washing with 100 μL of PBS, the cells were treated with 300 μL of 0.2% Triton X-100 in PBS at a flow rate of 20 μL/min for 15 min. After permeabilization, cells were treated with 3% BSA in PBS at a flow rate of 20 μL/min for 30 min. To identify CTCs and leukocytes, 600 μL of cell-staining solution containing 1 μg/mL of Hoechst 33342 (Molecular Probes); a cocktail of anti-pancytokeratin antibodies (Alexa488-AE1/AE3 (1:100 dilution; eBioscience, San Diego, CA, USA) and FITC-CK3-6H5 (1:60 dilution; Miltenyi Biotec, Auburn, California CA USA); and PE-labeled anti-CD45 antibody (1:120 dilution; BD Biosciences, San Jose, CA, USA) was flowed through the microcavities at a flow rate of 20 μL/min for 30 min. Finally, the array was washed with 400 μL of PBS containing 2 mM of EDTA and 0.5% BSA to remove any excess dye. After recovery of tumor cells, an image of the entire cell array area was obtained using a fluorescence microscope (BX61; Olympus Corporation, Tokyo, Japan) integrated with a 10× objective lens and a computer-operated motorized stage; WU, NIBA, and WIG filter sets; a cooled digital camera (DP-70; Olympus Corporation); and Lumina Vision acquisition software (Mitani Corporation, Tokyo, Japan).

In clinical trials, an entire image of the cell array area had been obtained using a fluorescence microscope (Axio Imager Z1; Carl Zeiss, Oberkochen, Germany) integrated with a 10× or 20× objective lens and a computer-operated motorized stage; WU, FITC, and Texas Red filter sets; a digital camera (AxioCam HRc; Carl Zeiss); and AxioVision acquisition software (Carl Zeiss). Subsequently, image analysis had been performed and objects that satisfied predetermined criteria had been counted. Fluorescent intensities and morphometric characteristics, such as cell size, shape, and nuclear size, were considered when performing CTC identification and non-tumor cell exclusion, with cells characterized by a round to oval morphology and a visible nucleus (i.e., as Hoechst-33342 positive) that were positive for cytokeratin and negative for CD45 identified as CTCs. Isolated CTCs on the transparent MCA were also stained using a May-Grünwald–Giemsa (MGG) staining method consisting of fixation with 4% PFA, undiluted May-Grünwald stain for 2 min, May-Grünwald stain diluted 50% in PBS for 1 min, and Giemsa stain for 18 min, followed by rinsing with PBS for 1 min.

CTC Enumeration using the CellSearch System

Whole blood samples were maintained at room temperature, mailed overnight to the laboratory of SRL Inc., and processed within 96 h of collection. All CTC evaluations were performed without knowledge of patient clinical status in the laboratory and

the results were reported quantitatively as the number of CTCs/7.5 mL of blood. CTCs were defined as EpCAM-isolated intact cells showing positive staining for cytokeratin and negative staining for CD45. In accordance with previous evaluations of the CellSearch system [8], a patient was considered CTC positive if ≥2 CTCs/7.5 mL of blood were detected in the patient's sample.

Results

CTC Isolation and Image Analysis using the MCA System

Isolation and staining of the tumor cells from whole blood was completed within 120–180 min, and image scanning of the MCA was performed at 3 fluorescence wavelengths using a 10× or 20× objective lens and a motorized stage. Figure 1b–f shows the scanning electroscope microscopy (SEM) and fluorescence images of the stained cells that were recovered on the MCA. As can be observed, solitary cells and cell clusters were individually trapped and retained on the microcavities that could be easily enumerated. Recovered cells that had a round to oval morphology and a visible nucleus (i.e., were Hoechst 33342 positive) and were positive for pancytokeratin and negative for CD45 were identified as tumor cells, while CD45-positive cells were identified as contaminating normal hematologic cells. The images reveal the existence of a distinct immunophenotype of epithelial cell marker-positive tumor cells. Although a number of leukocytes were retained on the array, tumor-cell enumeration was relatively facile because individual cells had been trapped on the precisely aligned microcavities.

Sensitivity of the MCA System in CTC Detection of Lung Cancer Cell Lines

In our previous study, varying numbers of cells of the lung cancer cell line NCI-H358 were spiked into blood, and tumor cell isolation was evaluated using our MCA system [31]. The calculated detection efficiency was constant and over 90% when 10–100 tumor cells were present per milliliter of blood. In this study, in order to evaluate the recovery efficiency of various lung cancer cell lines using the MCA system, 100 cells of each of 8 lung cancer cell lines (A549, HCC-827, NCI-H358, NCI-H441, PC-14, DMS-72, NCI-H69, and NCI-H82) were spiked into healthy donor blood samples and then processed by MCA assay. Table 1 shows the average recovery efficiency and typical diameter of the cell lines. As can be observed, a high recovery rate was obtained, regardless of tumor type, ranging from 68% to 100% in the cell line spike-in experiments. Most of the recovered cells were viable and able to proliferate even after undergoing the isolation process, suggesting the potential for further biological and molecular analysis of CTCs.

Next, in order to evaluate the specificity and sensitivity of CTCs detection, the sensitivity tests were performed on artificial samples prepared by adding 1 and 3 cultured NCI-H358 cells to healthy donor blood samples, as previously reported by Vona et al. [20]. One and 3 cultured NCI-H358 cells were spiked into separate 7.5 mL aliquots of blood. These 7.5 mL blood samples were processed with the MCA system in 3 independent tests (Table S1). The results demonstrated a sensitivity threshold for MCA system close to 1 tumor cell per 7.5 mL of blood. In addition, CTCs were not detectable from 6 healthy donor bloods using the MCA system (Figure 2). Therefore, a patient was considered CTC positive if ≥1 CTCs per 7.5 mL of blood was detected by the MCA system.

In addition, the tumor cell recovery efficiency of the MCA system was compared with that of ISET system (Figure S1). In this comparison, 100 cells of NSCLC cell line NCI-H358 was spiked into healthy donor blood samples and then processed by the MCA system and a track-etched polycarbonate 8-μm pore membrane (Nucleopore; Whatman Ltd., Kent, UK). The results revealed the recovery rate using the MCA system (100% ±5%) to be significantly higher than that using the ISET system (91% ±2%) ($p<0.05$, t-test), indicating that use of the MCA system enables CTC isolation with an efficiency equivalent to or greater than that of the ISET system.

Table 1. CTC recovery efficiency and average cell diameter.

Cell line	Origin	Average cell diameter (μm)	Recovery efficiency (%)
A549	NSCLC	17.3	98±3
HCC827	NSCLC	19.6	99±6
NCI-H358	NSCLC	18.1	100±6
NCI-H441	NSCLC	20.6	98±8
PC-14	NSCLC	19.5	97±2
DMS79	SCLC	14.1	76±1
NCI-H69	SCLC	12.5	68±2
NCI-H82	SCLC	13.5	80±4

Cells were spiked into 1 mL of normal blood and recovered using the MCA system.
doi:10.1371/journal.pone.0067466.t001

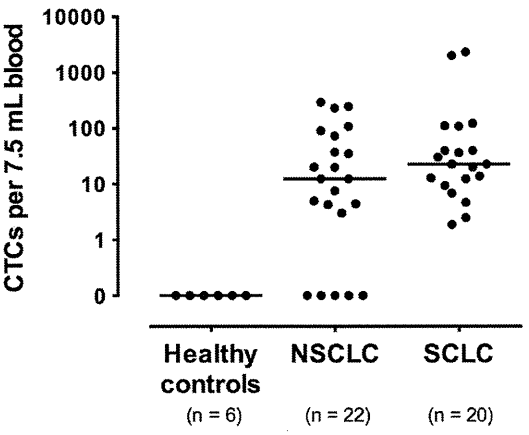

Figure 2. CTC count using the MCA system. CTC count/7.5 mL blood is shown for 6 healthy donors, 22 NSCLC patients and 20 SCLC patients.
doi:10.1371/journal.pone.0067466.g002

CTC Enumeration using the CellSearch System and the MCA System

To conduct blind comparison of the detection sensitivity of the CellSearch and MCA systems, blood samples were collected from 22 metastatic NSCLC and 21 SCLC patients between April 2011 and February 2012 and analyzed for determination of the number of patients identified as CTC positive by each system (Table 2). Of these samples, 1 sample collected from 1 SCLC patient was not evaluated by the MCA system because an insufficient volume of blood had been collected for processing by both systems. As a result, 17 of the 22 (77%) NSCLC patients were identified as CTC positive using the MCA system but only 7 of the 22 (32%) NSCLC patients using the CellSearch system (Table 3). Of these patients, 8 were identified as CTC positive by both the CellSearch system

and the MCA system, 1 was identified as CTC positive by the CellSearch system only, and 9 were identified as CTC positive by the MCA system only. Considering the results obtained by both systems together, 18 (82%) of the NSCLC patients were identified as CTC positive. Analysis of these findings revealed that a significantly greater number of NSCLC patients were identified as CTC positive by the MCA system (median cell count 13, range 0–291 cells/7.5 mL; Figure 2) than by the CellSearch system (median cell count 0, range 0–37 cells/7.5 mL), demonstrating the statistical superiority of the MCA system in CTC enumeration ($p = 0.0015$, Wilcoxon test; Table 3).

In contrast, 20 of the 20 (100%) SCLC patients were identified as CTC positive using the MCA system versus 12 of the 21 (57%) patients using the CellSearch system. The median CTC count was found to be 2 cells/7.5 mL (range 0–325) using the CellSearch system and 23 cells/7.5 mL (range 2–2329) using the MCA system (Figure 2). Although not reaching a level of statistical significance, the detection sensitivity of the MCA system in CTC enumeration showed a trend toward being greater than that of the CellSearch system ($p = 0.2888$, Wilcoxon test; Table 3). For each outcome, agreement between the test results of the systems was assessed by Bland–Altman plots [33]. In the analysis of agreement regarding CTC enumeration in NSCLC patients, the mean difference was 50.1 (95% CI, range 11.1–89.1), with the limits of agreement ranging from −125.8 to 226.0. The MCA system yielded disproportionally higher CTC counts at higher mean values compared to The CellSearch system (Figure S2a). In contrast, in the analysis of agreement regarding CTC enumeration in SCLC patients, the mean difference was 202.6 (95% CI, range −116.7–521.9), with the limits of agreement ranging from −1162.0 to 1567.2. Unlike with the analysis of NSCLC blood samples, no bias was observed between the systems in the analysis of SCLC samples except for subjects with extremely high CTC titer (Figure S2b). Statistical analysis also revealed no association between site of metastasis and the CTC count of lung cancer patients using either system (data not shown).

Table 2. Patient characteristics.

		NSCLC	SCLC
No. of patients		**22**	**21**
Gender	Male	10	18
	Female	12	3
Median age		68	73
	(Range)	(36–77)	(53–83)
Smoking	Smoker	16	21
	Never-smoker	6	-
ECOG-PS	0–1	16	13
	2–4	6	8
No. of organs with metastasis	Median	2	2
	(Range)	(1–6)	(1–5)
Metastasis	Brain	9	10
	Bone	8	4
	Liver	6	6
Histology	Adenocarcinoma	14	–
	Squamous	3	–
	Others	5	–
	SCLC	–	21

doi:10.1371/journal.pone.0067466.t002

Table 3. Comparison of CTC enumeration by the CellSearch system and the MCA system.

Sample ID		CellSearch CTC (cells/7.5 mL)	MCA CTC (cells/7.5 mL)
NSCLC	1	0	0
	2	0	0
	3	9	0
	4	0	0
	5	0	5
	6	0	8
	7	2	90
	8	0	13
	9	0	13
	10	0	3
	11	1	35
	12	37	20
	13	2	246
	14	18	108
	15	0	73
	16	10	231
	17	19	20
	18	1	4
	19	0	0
	20	0	4
	21	0	291
	22	0	38
SCLC	23	200	20
	24	189	30
	25	0	13
	26	0	9
	27	0	40
	28	0	7
	29	33	23
	30	2	14
	31	3	122
	32	18	2
	33	1	2329
	34	1	2021
	35	4	13
	36	15	5
	37	325	40
	38	2	–
	39	13	36
	40	110	110
	41	0	3
	42	0	23
	43	0	109

doi:10.1371/journal.pone.0067466.t003

Morphologic Features of CTCs Isolated using the MCA System

CTCs were counted, identified as being cytokeratin positive and CD45 negative, and as having a visible nucleus on the basis of analysis of fluorescent images. As can be observed in Figure 3, which shows a representative gallery of CTCs identified by image analysis, CTCs are larger than the surrounding leukocytes and often appear in clusters, defined here as contiguous groupings of cells containing 3 or more nuclei. Figure 4 shows a solitary CTC and a CTC cluster detected in one SCLC patient using the MCA system. Using the MCA system, CTC clusters were observed in 2 of the 22 NSCLC patients (Patient No. 13 and 21) and 4 of the 21 SCLC patients (Patient No. 31, 33, 34, and 43). May-Grünwald–Giemsa staining of the CTCs isolated using the MCA system revealed that they are characterized by a high N/C ratio, nuclear molding, and morphological similarity to primary tumor cells.

Discussion

ISET systems have been found to have higher CTC detection sensitivity than the CellSearch system in several cancers, including NSCLC [17,22] However, the pores of ISET filters, which are made of polycarbonate by track etching, are randomly placed within the systems at a nonuniform density. Unlike such track-etched polycarbonate filters, the size, geometry, and density of the microcavities in the MCA system assessed in the current study are precisely controlled to achieve specific cell separation according to differences in cellular size and deformability. Aligning cells on the MCA not only eases cell imaging by allowing for the scanning of specified areas with an automated fluorescence microscope but also enables reduction in the labor required for CTC counting [29,31]. As such, the MCA system provides a platform for the use of high-throughput imaging technologies that provide more rapid and less expensive data collection as well as CTC enumeration and advanced analysis of molecular phenomena, including fluorescence in situ hybridization for detection of tumor-specific genomic changes. Furthermore, the MCA is integrated with a miniaturized device so that enrichment of CTCs from blood, as well as staining and washing in the microfluidic assay, can be performed within one integrated device.

In the present study, CTCs isolated on the MCA were successfully stained with fluorescent-labeled antibodies that target tumor cell markers, and staining and washing were found to have little or no effect on the retention of tumor cells on the microcavities. Due to its very small size, the MCA system is portable, which, by enabling point-of-care CTC counting, eliminates the need to ship blood for testing under unfavorable shipment conditions and expedites clinical decision-making. These features, in addition to our recently developed procedure for isolating single cells from the MCA using microcapillaries, allow tumor cells to be recovered from the MCA for subsequent molecular analysis of CTCs [29].

In this blind comparison of use of the MCA system to that of the conventional CellSearch System for CTC enumeration in lung cancer patients, the MCA system was found capable of isolating various lung cancer cell lines spiked within whole blood at high levels of efficiency. However, the MCA system performed isolation of SCLC cell lines slightly less efficiently compared to that of NSCLC cell lines, indicating that small (<8 μm in diameter) cells of the SCLC cell lines might pass through the microcavities during blood filtration. In a previous study [31], we found that breast (MCF-7 and Hs578T), gastric (AGS and SNU-1), and colon (SW620) tumor cells lines that include EpCAM-negative tumor cells could be successfully recovered using the MCA system with greater than 80% efficiency. However, we also found that the efficiency of recovery of small cells (average diameter 11.6 μm) of the tumor cell line SW620 to be slightly less than that of other cell lines, as we did of the SCLC cell lines examined in this study.

The MCA system assessed in the present study was found to possess a higher detection sensitivity than the CellSearch system in NSCLC CTC enumeration, suggesting the superiority of size- and deformability-based isolation techniques compared to immuno-magnetic-based techniques. The poor sensitivity of CellSearch has been attributed to the low EpCAM expression in advanced NSCLC. However, one of the NSCLC patients assessed in the present study was found to be CTC positive using the CellSearch system but CTC negative using the MCA system, indicating that

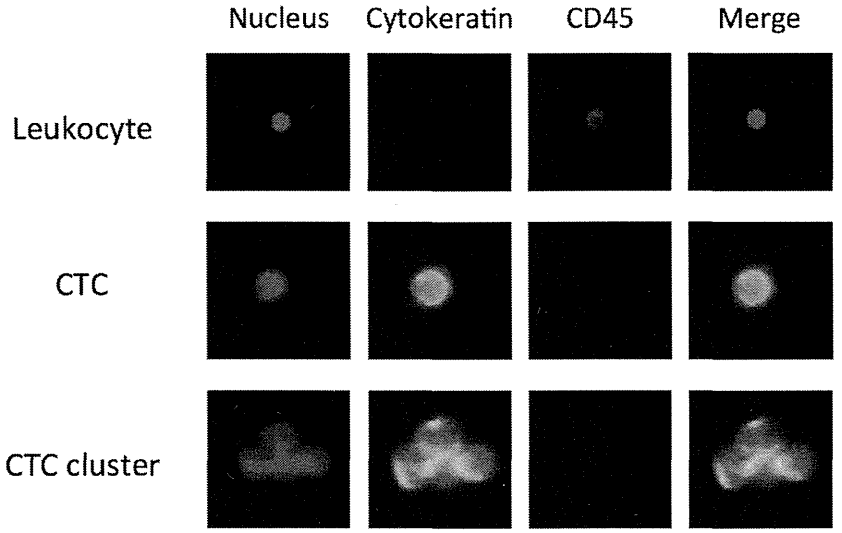

Figure 3. Gallery of cells captured on the MCA from blood of advanced lung cancer patients. Cells were stained with Hoechst 33342, FITC-labeled anti-cytokeratin antibody, and PE-labeled anti-CD45 antibody.
doi:10.1371/journal.pone.0067466.g003

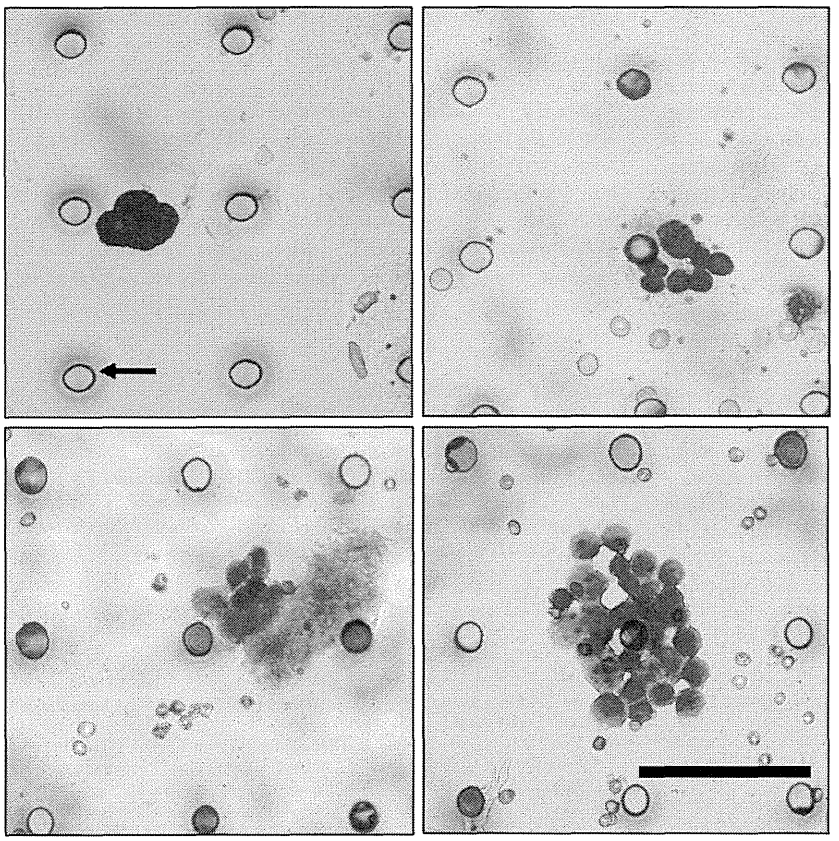

Figure 4. Gallery of CTCs captured on a transparent MCA from SCLC patient blood. May-Grünwald–Giemsa-stained cells showed a high nucleus–cytoplasm ratio and nuclear molding (×40). Black arrow indicates 9-μm microcavity. Scale bar = 60 μm.
doi:10.1371/journal.pone.0067466.g004

changes in EpCAM expression cannot solely account for the differences found between the two systems in NSCLC enumeration.

The CTC detection rate using the CellSearch system in SCLC patients was 67%, considerably higher than that in NSCLC patients and consistent with that found in previous studies [7,34–36]. Although the MCA system does not rely on EpCAM expression, which circulating SCLC cells have been reported to show high levels [37], in performing CTC isolation, its use was found to yield a high detection rate, indicating that it could be utilized for CTC detection in not only NSCLC but also SCLC patients. Nevertheless, the CTC counts of several patients were higher when analyzed using the CellSearch System compared to the MCA system, indicating that some small tumor cells in patient blood might flow through the microcavities, as described above. Previous research has suggested that immunomagnetic separation techniques lack the capacity to isolate large clusters, whereas use of size-based separation techniques leads to loss of small CTCs [17]. To address these problems, the shape of the microcavities in the MCA was modified to improve their efficiency in isolating small cells from tumor cells in whole blood in our recent study [38].

Observation of CTC clusters has been reported in various cancers, including lung cancer [23,24,39–42]. It is hypothesized that forming in clusters provides CTC cells with advantages over remaining solitary in terms of survival, proliferative capacity, and ability to form micrometastases. In this study, CTC clusters were isolated from both NSCLC and SCLC patients using the MCA system. Interestingly, the CTC-positive clusters were identified as having a small number of CTC cells by the CellSearch system but a large number by the MCA system. One reason why several SCLC patients were found to have a large CTC count when assessed by the MCA system may be that this system enables isolation of larger CTC clusters that cannot be isolated by immunomagnetic separation. Examination of this hypothesis requires further detailed analysis of the characteristics of CTC clusters, such as expression of epithelial markers and the presence of apoptotic cells within CTC clusters, which could be performed using the MCA system.

In conclusion, our results suggest that the MCA system is potentially superior to the CellSearch system in the CTC detection of lung cancer patients, with the former found capable of isolating significantly more CTCs and CTC clusters than the latter. The major limitation of this study was its examination of a small sample of patients with only one type of cancer. Further studies should thus examine larger cohorts of patients with various types of cancers to assess whether the MCA system is a more appropriate tool for CTC enumeration and characterization of metastatic tumors in patients with cancers other than lung cancer compared to other systems. We are currently planning the development of an automated MCA system that achieves robust, reliable, and reproducible sample processing for validation study using large cohorts of patients presenting at multiple institutes to assess the prognostic utility of CTC count in cancer patients.